Feary, D.A., Hine, A.C., Malone, M.J., et al., 2000
Proceedings of the Ocean Drilling Program, Initial Reports Volume 182

11. Site 1133[1]

Shipboard Scientific Party[2]

BACKGROUND AND OBJECTIVES

Site 1133 was located in 1037.2 m of water on the middle-upper slope of the Great Australian Bight (Fig. F1) and was designed primarily to address Cenozoic paleoceanographic objectives. The site was also situated to provide intermediate depth information as part of the overall shallow-to-deep drilling transect across the margin.

Site 1133 was located to intersect an expanded Neogene section that primarily consists of a thick interval (>1100 m) mapped as seismic Sequence 4 (Feary and James, 1998, reprinted as Chap. 2), overlain by a thinner (>250 m) interval of Sequence 3 (Fig. F2). Although other sites targeted these sequences to some extent (e.g., Site 1130 intersected Sequence 3, and Site 1132 intersected both Sequences 3 and 4), Site 1133 presented an opportunity to obtain a much-expanded record through these sequences. However, the expanded nature of the section at this location also carried the risk that lower parts of the section would not be cored if drilling penetration rates became too low to achieve these targets within a reasonable time. An excessive target depth (1727 m) was deliberately chosen for this site so that it could act as a fallback location should poor weather or bad drilling conditions rule out many of the other sites. Another consideration for site location was the need for an intermediate water depth site to recover equivalent intervals to horizons at the deepest water site (Site 1128) anticipated to lack calcareous fauna as a consequence of carbonate compensation depth (CCD) fluctuations.

A submarine canyon system occurs to the west of Site 1133 (Fig. F1), consisting of a broad canyon on the lower slope and narrow 'tributary' channels extending onto the upper slope. This system complicates seismic ties between this site and the other Leg 182 drill sites to the west and makes detailed seismic sequence assignment difficult. Nevertheless, sequence correlations were expected to be broadly correct, with the suc-

F1. Map showing Site 1133 in relation to other Leg 182 sites and the AGSO169 seismic lines, p. 18.

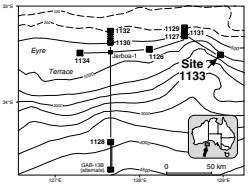

F2. Portion of seismic Line AGSO169/07a showing seismic stratigraphic sequences at Site 1133, p. 19.

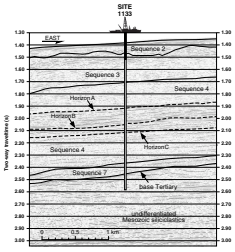

[1]Examples of how to reference the whole or part of this volume.
[2]Shipboard Scientific Party addresses.

Ms 182IR-111

cession expected to consist of a thin Pleistocene interval (<100 m), corresponding to seismic Sequence 2; an intermediate thickness (~260 m) of Sequence 3, expected to be of Pliocene age; and the considerably expanded Miocene section (>1100 m) of Sequence 4. In each case, the components of this succession were expected to provide deeper water facies information for comparison with shallower water equivalents at other sites. Despite approval for drilling through to the Paleogene (Sequence 7) and Cretaceous, there was no realistic expectation that these targets could be reached.

The broad objectives for Site 1133 were to

1. Recover pelagic ooze from the middle-upper slope as an intermediate water depth component of the Cenozoic paleoceanographic record of the opening of the Southern Ocean and the development of the Circum-Antarctic Current;
2. Determine the history of Cenozoic and Late Cretaceous CCD fluctuations and intermediate water-mass variations during the evolution of the Southern Ocean, in conjunction with Site 1128; and
3. Determine depositional and diagenetic facies within a Neogene succession in a middle to upper slope setting.

OPERATIONS

Transit to Site 1133

The 26-nmi sea voyage to Site 1133 required 3.0 hr at 8.7 kt. A beacon was dropped at 2200 hr on 26 November, initiating Site 1133.

Hole 1133A

The ship was stabilized on position and Hole 1133A was spudded at 0215 hr on 27 November. The bit was positioned at 1049 meters below rig floor (mbrf), and Core 1H recovered 9.78 m (Table T1). However, the excessive recovery was not appropriate for the establishment of a good mudline, and the hole was terminated.

T1. Site 1133 coring summary, p. 35.

Hole 1133B

The ship was not moved, the bit was repositioned at 1042 mbrf, and Hole 1133B was spudded at 0245 hr on 27 November. Core 1H recovered 2.40 m, indicating a water depth of 1037.2 meters below sea level (mbsl). Advanced hydraulic piston coring (APC) advanced to 50.9 meters below seafloor (mbsf), with Cores 3H–7H oriented and an Adara heat-flow measurement on Core 4H. The nonmagnetic core barrel assembly was run on Cores 3H, 5H, and 7H. Extended core barrel coring deepened the hole from 50.9 to 152.1 mbsf (Table T1). Recovery was very poor after Core 8X in mixed chert and unlithified bioclastic wackestones and packstones. While attempting to start the next core, the circulating pressure jumped to 2000 psi and the torque became erratic, indicating that the hole had caved in and was packing off the bit. The pipe was worked free, but the hole was judged unstable and operations at this hole were terminated. The bit cleared the seafloor at 2200 hr on 27 November, ending Hole 1133B.

Hole 1133C

The ship was moved 20 m south, and Hole 1133C was spudded at 2300 hr on 27 November. Core 1H was taken with the bit at 1045 mbrf and recovery was 5.74 m, indicating a water depth of 1036.8 mbsl. Advanced hydraulic piston coring advanced to 53.3 mbsf with 69.9% recovery (Table T1). The APC/extended core barrel and rotary core barrel (RCB) bottom-hole assemblies (BHAs) were inspected on the trip out, and no defects were noted. Both beacons were recovered, and the ship was secured for transit at 1330 hr on 28 November, ending Site 1133. A helicopter was dispatched to collect an ODP crew member because of a death in the family. The helicopter arrived at 1354 hr on 28 November and departed 2 min later, and the vessel was under way to return to Site 1129.

LITHOSTRATIGRAPHY

Introduction

Three major sedimentary units were recognized at Site 1133 and subdivided on the basis of major sediment type, texture, composition, color change, and presence of firmgrounds (Fig. F3). The upper sedimentary package consists of Pleistocene (see "Biostratigraphy," p. 7) pelagic calcareous ooze, and the middle sedimentary package is upper Miocene–lower Pliocene pelagic calcareous ooze. A lower, poorly recovered interval consists of lower–middle Miocene (see "Biostratigraphy," p. 7) neritic carbonate sediment. These deposits are unlithified to lithified bioclastic wackestone, packstone, grainstone, and chert/porcellanite (silicified limestone) (Fig. F3).

Recovery was more than 85% within the upper 35 mbsf of the cored interval, but then dropped abruptly because of the presence of unlithified to partially lithified bioclastic packstone interbedded with hard chert/porcellanite layers.

F3. Summary of lithostratigraphy, p. 20.

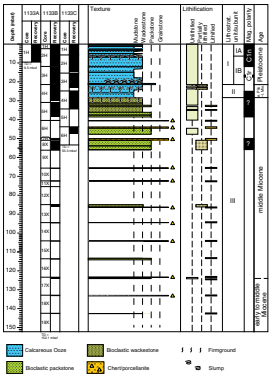

Lithostratigraphic Units

Unit I

Intervals: Core 182-1133A-1H; Core 182-1133B-1H through Section 4H-1, 9 cm; Core 182-1133C-1H through Section 3H-5, 106 cm
Depth: 0–9.78 mbsf (bottom of the hole; Hole 1133A); 0–21.49 mbsf (Hole 1133B); 0–22.36 mbsf (Hole 1133C)
Age: Pleistocene

Unit I consists of gray to light gray and white, moderately to strongly bioturbated calcareous ooze with varying amounts of calcareous nannofossils and planktonic foraminifers. Unit I is divided into two subunits based on color changes, textural differences, different patterns of sediment alternation, and the presence of firmgrounds in Cores 182-1133A-1H, 182-1133B-2H, and 182-1133C-2H.

Subunit IA

Intervals: Sections 182-1133A-1H-1 through 1H-5, 87 cm; Core 182-1133B-1H through Section 2H-3, 103 cm; Core 182-1133C-1H through Section 2H-1, 41 cm.

Depth: 0–6.87 mbsf (Hole 1133A); 0–6.43 mbsf (Hole 1133B); 0–6.21 mbsf (Hole 1133C)
Age: late Pleistocene

Subunit IA consists of light gray to gray, pale yellow, and white very fine grained calcareous ooze, characterized by a textural alternation between mudstone and wackestone, mostly as a result of variations in the proportion of planktonic foraminifers. The most conspicuous aspect of this subunit is the rapid variation in color. The lowermost bed in Subunit IA is a nannofossil ooze.

The matrix is dominated by calcareous nannofossils, common bioclasts, planktonic foraminifers, sponge spicules, and tunicate spicules (see **"Site 1133 Smear Slides,"** p. 25). Components of the sand-sized fraction (>63 µm) are dominant planktonic foraminifers and abundant to common bioclasts. Echinoid spines, ostracodes, and broken sponge spicules are also present. The abundance of benthic foraminifers varies from trace to common. Pteropod shields, gastropod shells, and large miliolid foraminifer tests are scattered throughout Subunit IA.

The sediment is moderately to strongly bioturbated throughout. Bioturbation is manifest as lighter to darker gray to pale olive color mottling. Burrows are filled by nannofossil foraminiferal ooze with a mudstone texture, or planktonic foraminiferal ooze with a wackestone texture. Burrows within the latter, with a diameter of as much as 3 cm, are interpreted as *Thallasinoides* ichnofossils. The lower boundary of Subunit IA lies at the base of a light gray nannofossil ooze containing planktonic foraminifers.

Subunit IB

Intervals: Sections 182-1133A-1H-5, 87 cm, through 1H-CC; Sections 182-1133B-2H-3, 103 cm, through 4H-1, 9 cm; Sections 182-1133C-2H-1, 41 cm, through 3H-5, 106 cm
Depth: 6.87–9.78 mbsf (bottom of the hole; Hole 1133A); 6.43–21.49 mbsf (Hole 1133B); 6.21–22.36 mbsf (Hole 1133C)
Age: Pleistocene

The upper boundary of Subunit IB is marked by a firmground as well as a change in lithology and color. Nannofossil ooze directly below the boundary contains well-defined burrows that are usually stiffer than the surrounding sediment, with a particularly large and deep *Thallasinoides* burrow in interval 182-1133A-1H-4, 85–145 cm. The lower boundary of Subunit IB is placed at the scoured base of a thin planktonic foraminiferal ooze turbidite (Fig. **F4**), above which is an interval of minor synsedimentary deformation interpreted as a slump. These boundaries are recognized in both Hole 1133B and Hole 1133C. The basal planktonic foraminiferal ooze has a grainstone texture and contains glauconite, bioclasts, and sponge spicules.

The main part of Subunit IB consists of silt to very fine grained nannofossil ooze and nannofossil planktonic foraminiferal ooze, with color alternations ranging from light olive gray to very light gray and white. This color change is rapid and dramatic, with contacts between colors generally burrowed. Sediment texture ranges from mudstone to wackestone. The matrix is dominated by nannofossils and abundant to common bioclasts (see **"Site 1133 Smear Slides,"** p. 25). Planktonic and benthic foraminifers and tunicate spicules are also present, as well as traces of dolomite. Most grains in the >63-µm fraction are very fine to fine-grained, abundant to dominant planktonic foraminifers, with

F4. Boundary between Units I and II, **p. 21.**

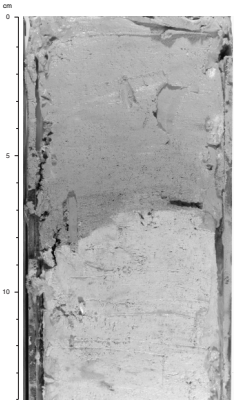

lesser benthic foraminifers and rare glauconite grains and blackened particles. Large benthic foraminifers are scattered throughout.

The sediment is moderately to strongly bioturbated, and burrows are commonly filled with packstone to grainstone of very fine to medium sand size composed of mainly planktonic foraminifers. Some burrows, 4–5 cm across and with diffuse outlines, are probably *Thallasinoides*.

The lower part of Subunit IB is slump folded (Fig. F5). Disharmonic and isoclinal folds are present, usually outlined by thin bands of white nannofossil ooze with a mudstone texture. All burrowing is considered to be preslumping.

F5. Inclined deformed beds in Hole 1133B, p. 22.

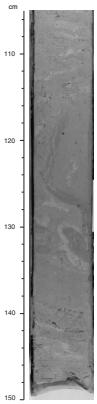

Unit II

Intervals: Sections 182-1133B-4H-1, 9 cm, through 4H-5, 115 cm; Sections 182-1133C-3H-5, 106 cm, through 4H-2, 130 cm
Depth: 21.49–28.55 mbsf (Hole 1133B); 22.36–30.60 mbsf (Hole 1133C)
Age: late Miocene–early Pliocene

The contact between Units I and II is an erosional surface at the top of a white nannofossil ooze with a mudstone texture that is overlain by light gray, grainy planktonic foraminiferal ooze in Cores 182-1133B-4H and 182-1133C-3H. This boundary is recognized in both Holes 1133B and 1133C. The fact that the sediments beneath this boundary are slightly more lithified suggests partial early marine cementation. The sediment texture is matrix supported (mudstone to wackestone). A minor firmground is recognized in Section 182-1133B-4H-2, 21 cm, but no lithologic change is present.

The major components of the matrix are calcareous nannofossils, together with planktonic and benthic foraminifers, tunicate spicules, and sponge spicules (see **"Site 1133 Smear Slides,"** p. 25). Dolomite rhombs are present in trace amounts. Components of the >63-µm fraction are abundant planktonic foraminifers, common sponge spicules, and minor glauconite grains. Macrofossils are rare throughout Unit II.

The sediments of Unit II are moderately to strongly bioturbated. Burrows also occur as diffuse color mottling throughout this subunit, but distinct burrows are visible. The sediment infillings in these burrows are coarser grained than the surrounding sediments. Such infilling sediments have a packstone texture, and many of the burrows are rich in pyrite grains.

Unit III

Intervals: Sections 182-1133B-4H-5, 115 cm, through 19X-CC; Sections 182-1133C-4H-2, 130 cm, through 6H-CC
Depth: 28.55–142.59 mbsf (bottom of the hole; Hole 1133B); 30.60–47.80 mbsf (bottom of the hole; Hole 1133C)
Age: early–middle Miocene

The boundary between Units II and III is a firmground at the top of an unlithified bioclastic wackestone that is overlain by white nannofossil ooze with a mudstone texture. This boundary is clearly recognized in Holes 1133B and 1133C.

Only the upper part of this unit was well recovered. The sediment is (1) gray to light gray, poorly sorted, unlithified bioclastic wackestone with very fine grained silt- to sand-sized particles; (2) gray, light gray to

light olive-gray, uniform, unlithified to partially lithified bioclastic packstone with poorly to well-sorted silt- to sand-sized grains; and (3) gray to dark gray chert/porcellanite (silicified limestone with wackestone texture). Most sediments recovered were fragmented during drilling. Some porcellanite/chert fragments are draped by a thin layer of unlithified to partially lithified bioclastic packstone. We infer that the entire unit of packstone and chert consists of these sediments, with beds or lenses of preferentially silicified limestone (formerly nannofossil planktonic foraminiferal ooze/chalk), forming the bulk of the material recovered.

The matrix of unlithified bioclastic wackestone contains calcareous nannofossils, bioclasts, traces of benthic foraminifers, clay, dolomite, and some rock fragments (see **"Site 1133 Smear Slides,"** p. 25). The coarse fraction (>63 µm) is dominated by bioclasts. Benthic and planktonic foraminifers are also present, as well as traces of echinoid spines and sponge spicules, all of which are overgrown by calcite cement. The coarse fraction (>63 µm) of unlithified to partially lithified bioclastic packstone contains dominant bioclasts, very small benthic foraminifers, sponge spicules, glauconite grains, and blackened grains.

Gray, fine-grained, laminated bioclastic grainstone and packstone/grainstone occurs in Cores 182-1133B-16X and 18X. Black particles and glauconite grains are present. Gray, fine-grained, silicified bioclastic packstone in interval 182-1133B-17X-CC, 0–16 cm, contains traces of planktonic foraminifers and glauconite grains. A thin section of Sample 182-1133B-17X-CC, 67–68 cm, contains 40% silt-sized dolomite rhombs (see **"Site 1133 Thin Sections,"** p. 26). The silicified limestone (porcellanite/chert) has a very fine to fine-grained wackestone texture, with distinct light gray to white burrows filled by lithified to partially lithified bioclastic wackestone and nannofossil foraminiferal chalk with a packstone texture.

Discussion

Recovery of Unit III was poor, and thus little information could be acquired regarding the sedimentary development of this part of the succession. Sediment composition indicates a mid-slope hemipelagic environment containing a mixture of pelagic particles and shelf-derived bioclasts. This interpretation is corroborated by the benthic foraminiferal assemblage, which indicates a middle to lower bathyal depositional setting for these deposits (see **"Biostratigraphy,"** p. 7).

A firmground forms the boundary between Units II and III, suggesting strongly reduced sedimentation rates. This level also coincides with a change to a more pelagic regime, as indicated by the calcareous ooze of Unit II. As a result, this firmground is interpreted as a flooding surface. Condensed sedimentation at the boundary between Units II and III is supported by the planktonic foraminiferal and calcareous nannofossil assemblage (see **"Biostratigraphy,"** p. 7).

An interruption of the pelagic sedimentation dominating during the Pleistocene is reflected by a slump in the basal part of Unit I. The redeposited sediments are calcareous ooze, indicating that middle Miocene deposits are not involved in the slump.

The remainder of Unit I consists of pelagic calcareous ooze. This middle and upper Pleistocene interval, however, is much reduced in thickness compared to other Leg 182 sites. Reduced sedimentation rates are also reflected by the firmground dividing Unit I. As Unit I corresponds to seismic Sequence 2, this firmground could represent the lateral

equivalent of the intra-Pleistocene flooding surface found at other sites (e.g., Site 1130).

BIOSTRATIGRAPHY

Introduction

Drilling at Site 1133 identified two major biostratigraphic units that were dated by nannofossils and planktonic foraminifers as Pleistocene and middle–early Miocene. The Pleistocene section extends down to 21.49 mbsf and includes a slump at the base from 19.9 to 21.4 mbsf. The unit overlies a thin, highly condensed interval with lower Pliocene–upper Miocene assemblages between two firmgrounds at ~23.5 and 29 mbsf. The upper firmground marks a hiatus of ~3 m.y. The firmground at 29 mbsf separates the lower Pliocene–upper Miocene (Zone NN12) from the middle Miocene (Zone NN6), an interval of ~6 m.y. Three main benthic foraminifer assemblages are recognized: a diversified Pleistocene calcareous assemblage, a diversified upper Miocene assemblage, and an impoverished middle–lower Miocene assemblage. All three assemblages indicate middle to lower bathyal paleodepths.

Calcareous Nannofossils

Calcareous nannofossils indicate that the stratigraphic sequence at Site 1133 consists of three main biostratigraphic units: a relatively thin Pleistocene section (~22 m thick) with moderately preserved assemblages (combined Zones NN21–NN20 and Zone NN19); a poorly preserved lower Pliocene–uppermost Miocene assemblage (Zone NN12) from a condensed section (~7 m thick, between 23.48 and 31.36 mbsf); and a relatively thick middle–lower Miocene section (>110 m thick) containing poorly to moderately preserved assemblages (Zone NN6 to combined Zones NN5–NN4).

The disconformity at the base of the Pleistocene at ~22 mbsf represents a hiatus equivalent to most of the Pliocene. Another hiatus of ~6 m.y. is suspected between the lower Pliocene–uppermost Miocene and the middle Miocene.

Pleistocene

Sample 182-1133B-1H-CC (2.37 mbsf) yielded an assemblage readily assignable to the combined Zones NN21–NN20. This assemblage contains *Gephyrocapsa caribbeanica, Helicosphaera carteri, Calcidiscus leptoporus,* small *Gephyrocapsa* spp., and *Umbilicosphaera sibogae*. Zone NN19 assemblages occur in Samples 182-1133B-2H-CC (11.8 mbsf) and 4H-1, 62–64 cm (22.02 mbsf). In addition to the key species *Pseudoemiliania lacunosa,* these assemblages include *Braarudosphaera bigelowii, C. leptoporus, Calcidiscus macintyrei, Coccolithus pelagicus, Dictyococcites productus, H. carteri, Reticulofenestra minutula, Reticulofenestra minuta, Rhabdosphaera clavigera,* and *Scyphosphaera* spp.

The Zone NN19 assemblage at 22.02 mbsf (Sample 182-1133B-4H-1, 62–64 cm) is followed downhole by a lower Pliocene–upper Miocene Zone NN12 assemblage at 23.48 mbsf (Sample 182-1133C-3H-CC), indicating a hiatus of ~3.3 m.y. Most of the Pliocene appears to be missing.

Pliocene–Miocene

The lower Pliocene–uppermost Miocene assemblage of Zone NN12 from Sample 182-1133C-3H-CC (23.48 mbsf) contains *Amaurolithus delicatus, Amaurolithus ninae, Discoaster brouweri, Discoaster pentaradiatus, Discoaster surculus, Discoaster variabilis,* and *Scyphospaera* spp., as well as *Discoaster barbadiensis* recycled from Eocene sediments. Assemblages from Samples 182-1133B-4H-CC (31.36 mbsf) through 7H-CC (50.72 mbsf) contain an association of species suggestive of Zone NN6, including *C. macintyrei, Calcidiscus premacintyrei, Reticulofenestra gelida,* and *Reticulofenestra pseudoumbilicus*. These assemblages also contain reworked species from older Miocene and Paleogene sediments (e.g., *Cyclicargolithus floridanus, Sphenolithus heteromorphus,* and *Dictyococcites bisectus*). A lithostratigraphic boundary at ~28 mbsf separates the assemblages of Zone NN12 from Zone NN6. A hiatus of ~6 m.y. is suspected at this boundary.

The key species for the combined Zones NN5–NN4, *S. heteromorphus,* consistently occurs from Sample 182-1133B-8H-CC (55.91 mbsf) down to the lowest section obtained from Hole 1133B (Sample 182-1133B-19X-H-CC at 142.56 mbsf). In addition to *S. heteromorphus,* assemblages from this thick section (~85 m) include *B. bigelowii, Dictyococcites antarcticus, C. premacintyrei, C. floridanus, H. carteri, Helicosphaera euphratis,* and *Sphenolithus moriformis*.

Planktonic Foraminifers

Sediments recovered at Site 1133 contain Pleistocene–middle Miocene planktonic foraminifer assemblages. The Pleistocene section extends down to ~21 mbsf and overlies a thin, highly condensed lower Pliocene–upper Miocene unit (22–28 mbsf). The disconformities at ~22 and ~28 mbsf represent hiatuses of ~3 and ~6 m.y., respectively. The underlying Miocene sediments are mainly of middle Miocene age, although poor preservation hampered the recognition of biozones.

Pleistocene

Well-preserved planktonic foraminifers of Pleistocene Zone Pt1 were found to 21.33 mbsf (Sample 182-1133B-3H-CC, 13–16 cm). Common species include *Globorotalia truncatulinoides, Globorotalia inflata, Globigerinoides ruber, Zeaglobigerina rubescens, Globigerina bulloides, Globigerina falconensis, Globigerina quinqueloba, Neogloboquadrina pachyderma,* and *Orbulina universa*. The entire interval probably represents mainly Subzone Pt1b, because the Subzone Pt1a index species *Globorotalia tosaensis* occurred only at 21.33 mbsf and immediately below, in Sample 182-1133B-4H-1, 4–6 cm (21.44 mbsf). The stratigraphic interpretation of this unit is complicated by a slump from 19.9 to 21.4 mbsf.

Early Pliocene–Late Miocene

The Pliocene Zone Pl1 assemblage is mainly composed of *Globorotalia crassaformis, Globorotalia puncticulata, Globorotalia margaritae,* and *Zeaglobigerina nepenthes,* and *Zeaglobigerina woodi,* as well as *G. falconensis, Globigerinita glutinata,* and *G. ruber.* This assemblage occurs between 21.44 and 23.48 mbsf in Samples 182-1133B-4H-1, 4–6 cm; 4H-1, 62–64 cm; and 182-1133C-3H-CC, 20–23 cm. The latter sample also contains *Globorotalia sphericomiozea, Globorotalia conomiozea,* and *Globigerinoides*

extremus, indicating a latest Miocene age. The occurrence of this Pliocene–upper Miocene assemblage in such a thin interval suggests that a large interval of time is not represented. The Pliocene–Pleistocene disconformity is ~3 m.y. above the first occurrence of *G. truncatulinoides* and the first appearance datum of *G. crassaformis* (<2–4.5 Ma).

Middle Miocene

Poorly preserved planktonic foraminifers, indicating mainly middle Miocene age, were recorded in the interval from ~31 to 123 mbsf (Samples 182-1133B-4H-CC through 17X-CC). This biofacies change coincides with the lithostratigraphic Unit II/Unit III boundary at ~28 mbsf (see **"Lithostratigraphy,"** p. 3). A middle Miocene age is indicated by the association of *Globoquadrina dehiscens, Globoconella conoidea, G. panda, Neogloboquadrina nympha, O. universa,* and *Fohsella peripheroronda*. However, the occurrence of upper Miocene species *Globorotalia conomiozea, Globorotalia menardii,* and *Globorotalia plesiotumida* (Samples 182-1133B-4H-CC, 11–14 cm, and 5H-CC, 8–11 cm) is puzzling. These younger taxa are probably downhole contamination. If this is the case, the disconformity at ~28 mbsf, between this middle Miocene section and the overlying thin Pliocene–upper Miocene unit, represents a hiatus of ~6 m.y. with most of the lower part of the upper Miocene missing. Postcruise studies, however, are needed to clarify this assertion. Further downhole, the two chert samples from the base of Hole 1133B (Samples 182-1133B-18X-CC, 30–33 cm, and 19X-CC, 6–9 cm) contain no diagnostic planktonic foraminifers; however, the samples do contain nannofossils of the combined Zones NN4–NN5 of the early–middle Miocene (see **"Calcareous Nannofossils,"** p. 7) (Fig. F6).

F6. Calcareous nannofossil and planktonic foraminifer zones, and benthic foraminifer assemblages, p. 23.

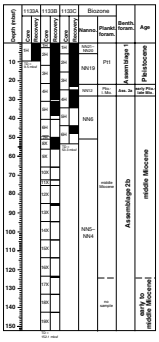

Benthic Foraminifers

Benthic foraminifers were studied from all core-catcher samples from Hole 1133B. Additional samples were examined from intervals in which marked lithologic change occurred. Benthic foraminifers are generally abundant in the upper part of Hole 1133B (Cores 1H through 4H). Abundance decreases significantly and preservation deteriorates below Core 182-1133B-4H. Between 100 and 300 benthic foraminifers were picked from the >63-µm fraction, except in samples in which abundance was low. The following benthic foraminifer assemblages, containing mainly cosmopolitan taxa, are recognized in the Cenozoic succession at Site 1133.

Assemblage 1 (Pleistocene)

Cores 182-1133B-1H through 3H

This relatively diverse assemblage is characterized by *Laticarinina pauperata, Hoeglundina elegans, Martinottiella communis, Plectofrondicularia vaughni, Anomalinoides globulosus, Bulimina aculeata, Eggerella bradyi, Pyrgo murrhina, Sphaeroidina bulloides, Planulina wuellerstorfi, Uvigerina hispidocostata, Sigmoilina obesa, Globocassidulina subglobosa, Sigmoilopsis schlumbergeri, Cibicidoides mundulus, Migros* sp., *Loxostomoides* spp., *Nodogenerina* spp., *Anomalinoides* spp., and various nodosariids. Middle to lower bathyal paleodepths are suggested by the presence of the depth indicative species *S. schlumbergeri, Eggerella bradyi, P. wuellerstorfi, P. murrhina,* and *P. vaughni*.

Assemblage 2A (Pliocene–Late Miocene)

Interval 182-1133B-4H-1, 10 cm, through 4H-5, 115 cm

This well-preserved, relatively diverse assemblage occurs within Core 182-1133B-4H in a discrete lithostratigraphic unit (see "Lithostratigraphy," p. 3) representing a condensed interval of early Pliocene–late Miocene age, bounded by two disconformities. The assemblage in Sample 182-1133B-4H-1, 62–64 cm, includes taxa characteristic of Assemblage 1. However, the sample contains a higher abundance of *P. wuellerstorfi,* lower abundance of *Nodogenerina* spp., and lacks *H. elegans, Migros* spp., and *Loxostomoides* spp. Middle to lower bathyal paleo-depths are indicated by the overall composition of the assemblage.

Assemblage 2B (Middle Miocene)

Interval 182-1133B-4H-5, 115 cm, through 15H-CC

This poorly preserved, impoverished assemblage is found in an interval of poor core recovery, from which mostly chert fragments were recovered. The assemblage consists mainly of *Stilostomella* spp., *Bolivina* spp., and *Cibicidoides* spp. However, Sample 182-1133B-5H-CC contains a slightly more abundant and diverse assemblage than the core-catcher samples below. The assemblage also comprises *S. bulloides, Vulvulina spinosa, Eggerella bradyi, Rectuvigerina striata, A. globulosus, Siphonina tenuicarinata, Trifarina* spp., *Tritaxia* spp., and various nodosariids. A few abraded tests of *Patellina corrugata* and *Elphidium* spp. within Sample 182-1133B-5H-CC suggest reworking and redeposition from shallower depths. Middle to lower bathyal paleodepths are tentatively proposed for this interval, which lacks distinctive bathymetric indicators. Further work will clarify the paleobathymetry of this interval.

Sedimentation Rates

Sediment accumulation rates were calculated from preliminary biostratigraphic and paleomagnetic data from Site 1133 and the results are presented in Figure F7. The datum levels used to calculate sedimentation rates are listed in Table T2. Slow sedimentation rates of ~9–16 m/m.y. are calculated for the Pleistocene, in comparison with the high sedimentation rates averaging between ~240 m/m.y. and ~31 m/m.y. in coeval sections at Sites 1127 and 1126, respectively. A disconformity representing a hiatus of ~3 m.y. separates the Pleistocene from an upper Miocene condensed interval at ~21 mbsf. A second disconformity at 28.55 mbsf separates upper Miocene (Zone NN12) from middle Miocene (combined Zones NN5–NN4), a hiatus of ~6 m.y. High sedimentation rates of 50 m/m.y. are indicated for the remainder of the lower–middle Miocene succession. However, sedimentation rates for this site remain tentative and should be treated with caution because of the scarcity of reliable datum levels.

F7. Sedimentation rate curve from datum levels for Site 1133, p. 24.

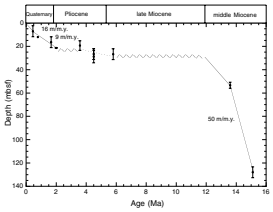

T2. Datum levels used in the graph of sedimentation rate, p. 37.

PALEOMAGNETISM

Shipboard paleomagnetic measurements in Holes 1133B and 1133C consisted of long-core measurements at 5- to 10-cm intervals of the natural remanent magnetization (NRM) and the remanence after alternating field (AF) demagnetization at 20 mT, as described in "Paleo-

magnetism," p. 12, in the "Explanatory Notes" chapter. Long-core measurements established a tentative Pleistocene magnetostratigraphy to a depth of ~30 mbsf in Hole 1133B, which includes the Brunhes (0–12 mbsf), Matuyama (12–24 mbsf), and Gauss (24–? mbsf). The interpretation is problematic because the same result was not reproduced in Hole 1133C, which yields uniform normal polarity magnetizations to a depth of 20 mbsf and anomalously shallow magnetizations of both polarities below this depth.

Long-Core Measurements

Intensity of the NRM is very low, with a median of ~1.5 × 10^{-4} A/m. High values are observed in the uppermost 5 mbsf, although the highest intensities (and susceptibilities) are observed in a package composed of wackestones, observed in both holes at ~30 mbsf. The NRM inclinations are predominantly of moderately positive inclination (Fig. F8). After partial demagnetization (20 mT), inclinations in Hole 1133B define intervals of negative and positive inclination. In contrast, the record for Hole 1133C yields magnetizations of predominantly negative inclination to a depth of ~20 mbsf, at which point inclinations are shallow and no meaningful polarity record can be obtained. Declinations in both holes are scattered about 0°/360°, the direction of the fiducial line in sample coordinates. This probably reflects the acquisition of a drilling-induced remanence. Measurements on discrete samples were unsuccessful because of the overall low intensity of the remanence.

F8. Downhole inclination with interpreted magnetostratigraphy, p. 25.

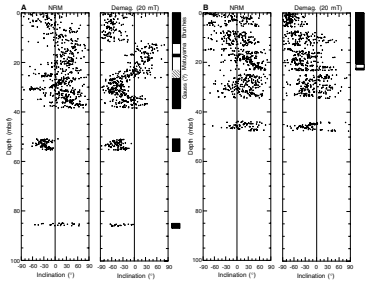

Rock Magnetism

Rock magnetism analysis consisted of measurements of weak-field susceptibility at two frequencies, progressive isothermal remanent magnetization (IRM) acquisition, and AF demagnetization of anhysteretic remanent magnetization (ARM). Decay of the NRM upon AF demagnetization is typical of a cubic phase, either magnetite or greigite. Representative samples were given a 400-mT IRM and subsequently demagnetized (Fig. F9). Inductions of 400 mT were not sufficient to reach saturation, suggesting that magnetic sulfides are present and may be important remanence carriers. Alternating field decay of the IRM suggests that in some of the cored intervals, contributions from single-domain size particles is less important than that from multidomain particles (Cisowski, 1981). This is also manifest in the lower ARM:IRM ratios observed at this site (<0.1). Magnetic susceptibility is of low negative values and is therefore dominated by the contributions of the diamagnetic carbonate matrix.

F9. Demagnetization of NRM, ARM, and IRMs, and of the acquisition of IRM, p. 26.

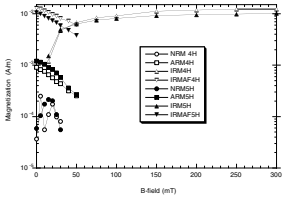

Magnetostratigraphy

The long wavelength pattern of normal polarity from 0 to ~12 mbsf, reversed polarity from 12 to ~24 mbsf, followed by a return to dominantly normal polarity appears to be a manifestation of the Brunhes-Matuyama-Gauss, Pliocene–Pleistocene sequence, lacking a good definition of the Jaramillo and Olduvai normal zones in the Matuyama (Fig. F8). As noted above, this interpretation is problematic because the same result was not reproduced in Hole 1133C. Therefore, possible correlation with the geomagnetic polarity time scale in the Pliocene–Pleistocene is uncertain.

COMPOSITE DEPTHS

Introduction

Construction of the composite and spliced section from Holes 1133B and 1133C followed the methods outlined in "Composite Depths," p. 14, in the "Explanatory Notes" chapter. Table T3 (also in ASCII format) relates mbsf depth to meters composite depth (mcd) for each core and section at Holes 1133B and 1133C and provides offset values for the conversion of mbsf depths to mcd. The composite section indicates full recovery to a depth of 42 mcd.

T3. Site 1133 core and section depths in mcd and mbsf, p. 38.

Data Input

The primary lithologic parameters used to create the composite section were the 400-nm color reflectance data, a ratio of the 700- to 400-nm color reflectance data measured on split cores, and gamma-ray attenuation (GRA) density data measured on whole-round cores (Fig. F10). For specifics regarding data collection procedures and parameters, see "Physical Properties," p. 14. Biostratigraphic and paleomagnetic datums were not used in the construction of the composite section because of the shallow total depth of coring and the disturbance of the record caused by slumping.

F10. Composite depth section produced using Splicer software, p. 27.

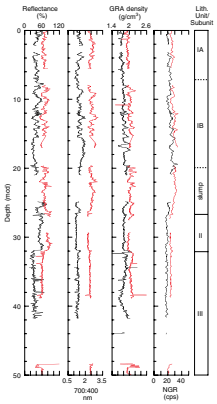

Composite Section Construction

The composite section for Site 1133 is presented in Figure F10. The primary difficulty encountered in the construction of this composite section was the presence of a slumped interval from 19.9 to 27 mcd in both holes and poor recovery below 38 mbsf resulting from the presence of multiple chert beds.

The sediments comprising the composite section range from Holocene to middle Miocene age, based upon biostratigraphic data (see "Biostratigraphy," p. 7). The stratigraphic record within the range of the composite section is divided into three primary lithostratigraphic units. The upper unit, lithostratigraphic Unit I, is further divided into two subunits. Subunit IA (0–6 mbsf) is defined by the presence of thinly interbedded unlithified calcareous ooze mudstones and wackestones, which exhibit distinctive but low-amplitude features in the color reflectance and density data that are easily correlated between holes. Lithostratigraphic Subunit IB (6–21 mbsf) consists of thicker beds (4–6 m) of calcareous ooze mudstone and wackestone, which are easily correlated on the basis of distinctive, high-amplitude, 2- to 5-m-thick oscillations in the color reflectance and GRA density records (Fig. F10).

A slumped calcareous ooze unit occurs near the base of lithostratigraphic Unit 1 from ~19.9 to 26.5 mcd. The top of the slumped interval was picked and correlated between holes using the occurrence of multiple very short wavelength (<0.5 m), high-amplitude excursions in the color reflectance data (Fig. F10) that correspond to distorted, alternating bands of light and dark color in the slumped sediments. The base of the slump was correlated between holes at a prominent transition to a plateau in high reflectance values and low 700:400 nm and GRA density values. These data characteristics correspond to lithostratigraphic Unit II, a calcareous ooze of early Pliocene–late Miocene age. The base of lithostratigraphic Unit II was correlated between holes at a prominent decrease in reflectance values and an increase in density values at

32 mcd. This transition corresponds to a major unconformable surface separating lithostratigraphic Unit II from darker bioclastic wackestones of lithostratigraphic Unit III (middle Miocene).

The composite and spliced sections indicate that recovery was complete to 42 mcd. (Figs. F10, F11; Table T4, also in ASCII format). Minimal recovery in cores below 42 mcd prohibited further composite section construction.

ORGANIC GEOCHEMISTRY

At Site 1133, in addition to routine monitoring of hydrocarbon gases for safety, inorganic carbon analyses were made. The analytical procedures are described in "Organic Geochemistry," p. 16, in the "Explanatory Notes" chapter.

Volatile Hydrocarbons

Concentrations of volatile hydrocarbons were routinely determined in every core from Holes 1133A and 1133B using standard ODP headspace sampling procedures. With the exception of two samples, only low concentrations of methane were detected; the maximum concentration was 170 ppm, with most samples having <12 ppm (Table T5). No heavier (C_{2+}) hydrocarbon gases were detected.

Inorganic and Organic Carbon, Sulfur, and Nitrogen

Calcium carbonate content in Holes 1133A and 1133B ranges from 78.5 to 94.4 wt%; most samples have 85 to 92 wt% (Table T6; Fig. F12).

Organic carbon (C_{org}) is low at Site 1133. Concentrations of C_{org} are all <0.4 wt%, and about half the samples have <0.2 wt% (Table T6; Fig. F12).

Sulfur concentrations range as high as 0.36 wt%, with about half the samples having no detectable sulfur. Nitrogen is present in only five samples, and concentrations range from 0.05 to 0.20 wt%.

INORGANIC GEOCHEMISTRY

Interstitial Waters

Interstitial water (IW) samples from Hole 1133B were taken at a rate of one per core for the first five cores. As a result of poor recovery, further sampling was restricted to Cores 182-1133B-8X and 17X. No samples were taken from Hole 1133A. Samples were analyzed according to the procedures outlined in "Inorganic Geochemistry," p. 18, in the "Explanatory Notes" chapter. The data are presented in Table T7 and Figures F13 and F14.

Salinity and Chlorinity

Salinity and chlorinity values increase with depth, reaching a maximum concentration of 41 and 662 mM, respectively, at 123.4 mbsf (Fig. F13). This increase of both values suggests that, as at the previous sites, a brine may exist below the cored interval.

F11. Spliced section of color reflectance data and NMR data produced using Splicer software, p. 28.

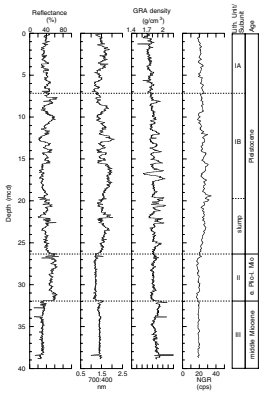

T4. Site 1133 splice tie points, p. 39.

T5. Headspace gas compositions, Hole 1133B, p. 40.

T6. $CaCO_3$, C_{org}, N, and S data, p. 41.

F12. $CaCO_3$ and C_{org} contents in samples, p. 29.

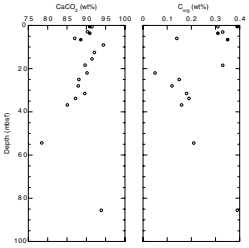

T7. Interstitial water geochemistry, p. 42.

F13. Concentration depth profiles of salinity, Cl^-, Ca^{2+}, Mg^{2+}, K^+, and Sr^{2+}, p. 30.

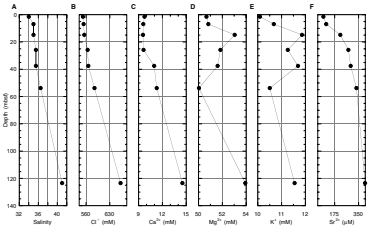

Calcium, Magnesium, Strontium, Potassium, Silica, and Iron

As a result of the increasing salinity, the concentrations of Ca^{2+}, Mg^{2+}, K^+, and Sr^{2+} generally increase with depth (Fig. F13). Calculation of the excess concentration normalized to chlorinity, however, shows that as much as 8.9 mM of Mg^{2+} are lost from the pore fluids at 123.4 mbsf. This depletion most likely results from recrystallization processes involving the uptake of Mg^{2+}. As a result of opal-A dissolution, silica values increase with depth and reach a maximum of 702 µM at 123.4 mbsf. Iron occurs only in minor amounts; the highest concentration, 6.6 µM, was measured from 25.8 mbsf.

Sulfate and Alkalinity

As a result of the increasing salinity with depth, sulfate concentration increases from 27.4 mM to a maximum concentration of 29.3 mM at 123.4 mbsf (Fig. F14). Normalization of the SO_4^{2-} concentration to Cl^- shows that as much as 4.8 mM of sulfate has been removed by a depth of 123.4 mbsf. The relatively small increases in alkalinity suggest that most of the 9.6 mM of alkalinity, which should have been produced by sulfate reduction, was precipitated as calcite or dolomite.

X-Ray Mineralogy

As with the IW samples, only the first five cores and Cores 182-1133B-8X and 13X were sampled. The recovered samples show a considerable change in the ratio of low-Mg calcite (LMC) to high-Mg calcite (HMC) ratio (Table T8, also in ASCII format), which is possibly a result of facies changes. However, because of the slow sedimentation rate, even slow diagenetic changes may cause a considerable change in the LMC/HMC ratio (Table T8).

PHYSICAL PROPERTIES

Introduction

Measurements of physical properties at Site 1133 followed the procedures outlined in "Physical Properties," p. 19, in the "Explanatory Notes" chapter. These included nondestructive measurements of *P*-wave velocity (every 4 cm; Table T9, also in ASCII format), GRA bulk density (every 4 cm; Table T10, also in ASCII format), magnetic susceptibility (MS) (every 8 cm; Table T11, also in ASCII format), and natural gamma radiation (NGR) (every 16 cm; Table T12, also in ASCII format) using the multisensor track (MST). The *P*-wave logger was activated only on APC cores. A minimum of four discrete *P*-wave velocity measurements per section were made on the working half of the split cores (Table T13, also in ASCII format). Standard index properties (Table T14, also in ASCII format) and undrained shear strength (only in unconsolidated sediments) (Table T15, also in ASCII format) were measured at a frequency of one per section. Thermal conductivity was measured in unconsolidated sediment at a frequency of one per core (Table T16, also in ASCII format). Difficulties occurred with the pycnometer used for determination of dry volume for index properties measurements (see "Index Properties," p. 21, in the "Explanatory Notes" chapter).

F14. Concentration depth profiles of $H_4SiO_4^0$, Li^+, Fe^{2+}, NH_4^+, SO_4^{2-}, pH, and alkalinity, p. 31.

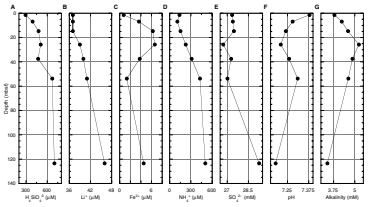

T8. XRD data, p. 43.

T9. *P*-wave velocity measurements, p. 44.

T10. GRA densiometry measurements, p. 45.

T11. Magnetic susceptibility measurements, p. 46.

T12. Natural gamma-ray measurements, p. 47.

T13. Discrete *P*-wave velocity measurements, p. 48.

T14. Index properties measurements, p. 49.

T15. Undrained shear-strength measurements, p. 50.

T16. Thermal conductivity measurements, p. 51.

The following sections describe the downhole variations in sediment physical properties and their relationships to lithology and downhole logging measurements. Variations in MS are described within "Paleomagnetism," p. 10.

Index Properties, *P*-Wave Velocity, Natural Gamma Radiation, and GRA Densiometry

An offset was seen between discrete bulk density measurements and the GRA densiometry measurements of the MST (Fig. F15). This offset was corrected using the equation of Boyce (1976), as described in "Index Properties," p. 21, in the "Explanatory Notes" chapter. Physical properties measurements at Site 1133 were limited because of poor core recovery. Despite this, data from Site 1133 closely reflect lithologic variations observed in the recovered sediments, and these data can be divided into two units with the boundary corresponding to the base of the Pleistocene section (see "Biostratigraphy," p. 7) (Fig. F15).

Physical properties Unit (PP Unit) 1 (0–21.8 mbsf), which corresponds to lithostratigraphic Subunits IA and IB (see "Lithostratigraphy," p. 3), is characterized by increasing NGR to 19.5 mbsf (5–22 cps) and then a sharp decrease to the base of the unit (Fig. F15). This NGR profile may be diagenetic in origin, as the base of PP Unit 1 is correlated with the loss of aragonite and HMC in the sedimentary section (see "Inorganic Geochemistry," p. 13). Bulk density (1.65–1.95 g/cm³) and velocity (1.57–1.62 km/s) exhibit high variability but generally increase downward throughout PP Unit 1, as porosity decreases from ~62% to ~45% (Fig. F15). These trends result from an overall increase in lithification with depth in lithostratigraphic Unit I (see "Lithostratigraphy," p. 3). At the base of PP Unit 1, bulk density decreases to 1.8 g/cm³ and porosity increases to 53%. The lower boundary of PP Unit 1 correlates with a firmground marking the base of lithostratigraphic Unit IB (see "Lithostratigraphy," p. 3).

The upper 6.2 m of PP Unit 2 (21.8–152.1 mbsf) is composed of calcareous ooze characterized by decreasing grain size and increasing lithification with greater depth. This change is reflected in the physical properties data as a decrease in NGR (9–5 cps) and bulk density (1.8–1.7 g/cm³) and an increase in porosity (52%–59%) (Fig. F15). The upper/middle Miocene boundary and the upper limit of lithostratigraphic Unit II occur at 28 mbsf and are marked by a firmground and the downcore appearance of neritic carbonates (see "Lithostratigraphy," p. 3). This lithostratigraphic boundary corresponds to an increase in bulk density and shear strength (Fig. F15), although it is not a major physical properties boundary. The remainder of PP Unit 2 is characterized by low NGR values (~5 cps) and variable density and *P*-wave velocity. This variability is the result of alternations between silicified limestones and partially lithified/unlithified packstones (see "Lithostratigraphy," p. 3). The lack of recovery in this interval hinders the complete characterization of this unit.

F15. Core recovery, NGR, bulk densities, *P*-wave velocity, porosity, and MS measurements, p. 32.

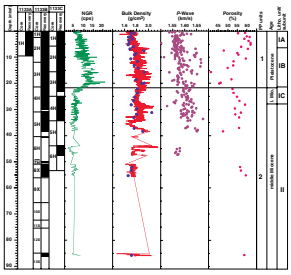

Shear Strength

Undrained peak and residual shear strength were measured on unconsolidated sediments from 0 to 47 mbsf (Fig. F16). Shear strength increases downhole from 5 to 26 kPa as a result of compaction, punctuated by increased variability within PP Unit 2 (Fig. F16). This variabil-

F16. Shear strength data, p. 33.

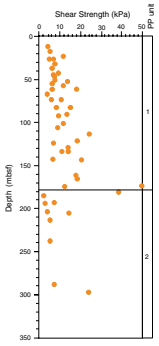

ity is, in part, caused by alternations in sediment lithification. However, in some intervals, shear strength variability may also result from drilling disturbance and cracking of the sediment before sediment failure, producing lower values for peak strength.

Thermal Conductivity

Thermal conductivity measurements were made from 0 to 76 mbsf at Site 1133. Values increase throughout PP Unit 1 from 0.985 to 1.215 W/(m·K) (Fig. **F17;** Table **T16**). Within PP Unit 2, thermal conductivity decreases from 1.21 to 1.01 W/(m·K) (Fig. **F17**). This trend is likely to be biased by the low recovery within the unit. In general, thermal conductivity data correlate well with other sediment physical properties, particularly bulk density.

F17. Thermal conductivity and bulk density data with PP units, **p. 34.**

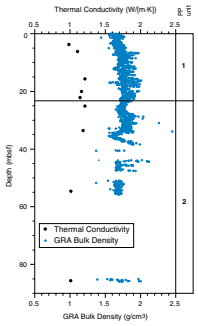

REFERENCES

Boyce, R.E., 1976. Definitions and laboratory techniques of compressional sound velocity parameters and wet-water content, wet-bulk density, and porosity parameters by gravimetric and gamma-ray attenuation techniques. *In* Schlanger, S.O., Jackson, E.D., et al., *Init. Repts. DSDP,* 33: Washington (U.S. Govt. Printing Office), 931–958.

Cisowski, S., 1981. Interacting vs. non-interacting single domain behavior in natural and synthetic samples. *Phys. Earth Planet. Inter.,* 26:56–62.

Feary, D.A., and James, N.P., 1998. Seismic stratigraphy and geological evolution of the Cenozoic, cool-water, Eucla Platform, Great Australian Bight. *AAPG Bull.,* 82:792–816.

Figure F1. Map showing the location of Site 1133 on the central Great Australian Bight middle-upper slope in relation to the other Leg 182 sites and the Australian Geological Survey Organisation Survey 169 (AGSO169) seismic lines.

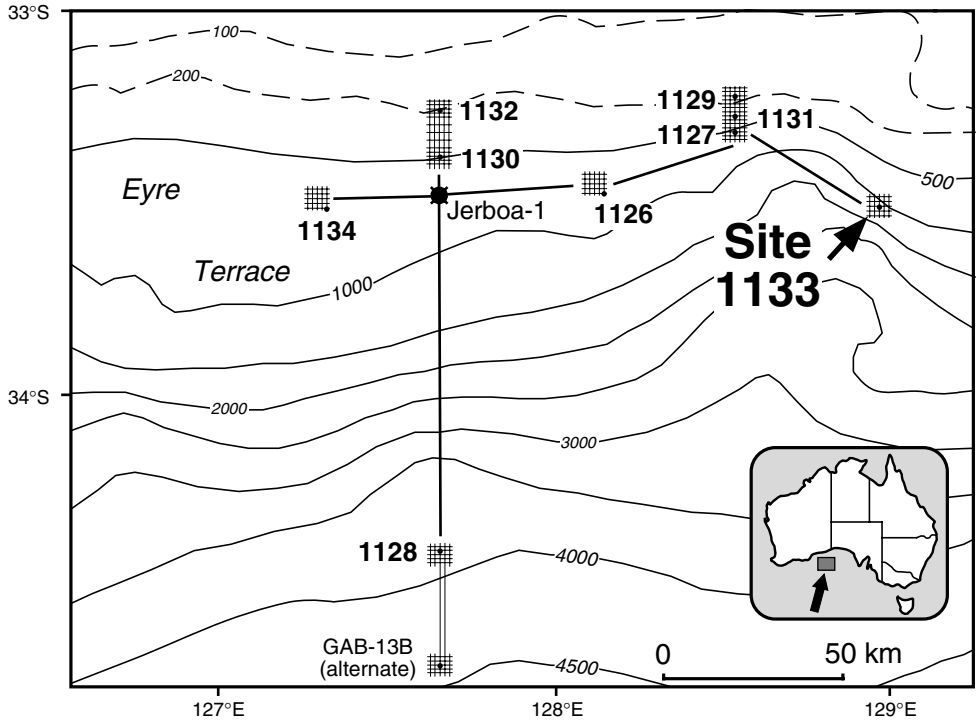

Figure F2. Portion of seismic Line AGSO169/07a showing interpreted seismic stratigraphic sequences planned (shown in white) and actually intersected (shown in black) at Site 1133.

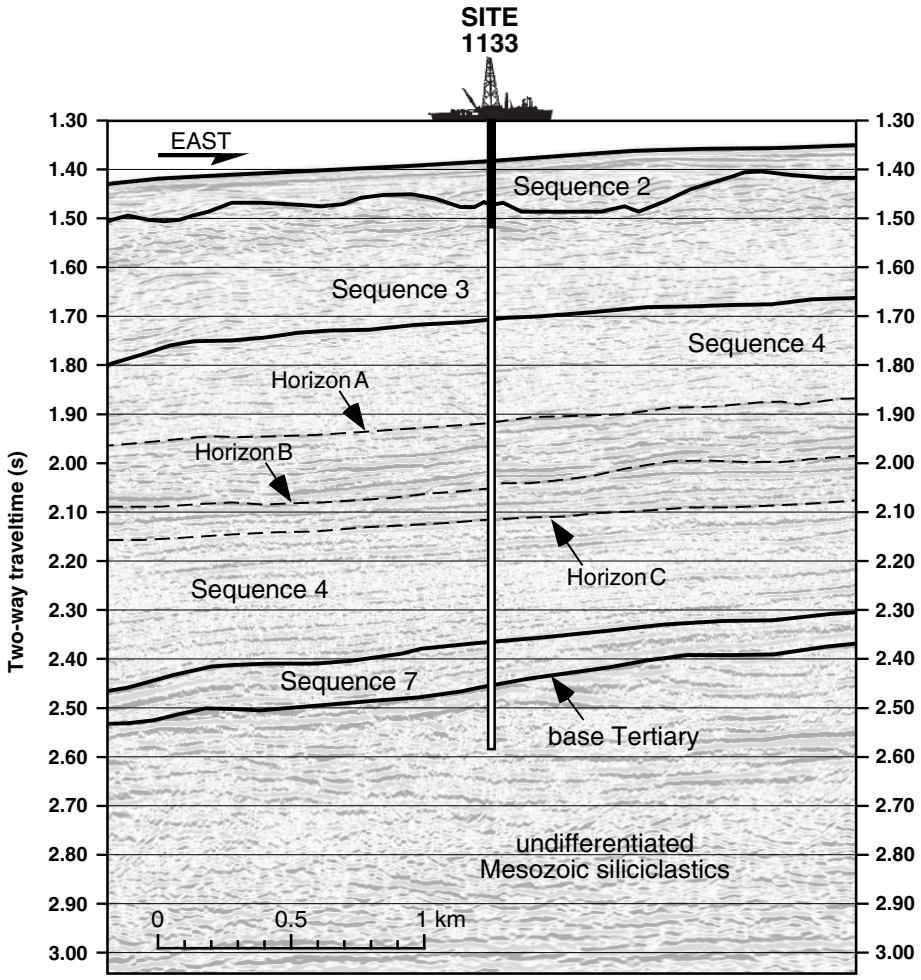

Figure F3. Summary of lithostratigraphy, Site 1133. ? = magnetic intensity too low to measure. Magnetostratigraphy and age are taken from **"Paleomagnetism,"** p. 10, and **"Biostratigraphy,"** p. 7.

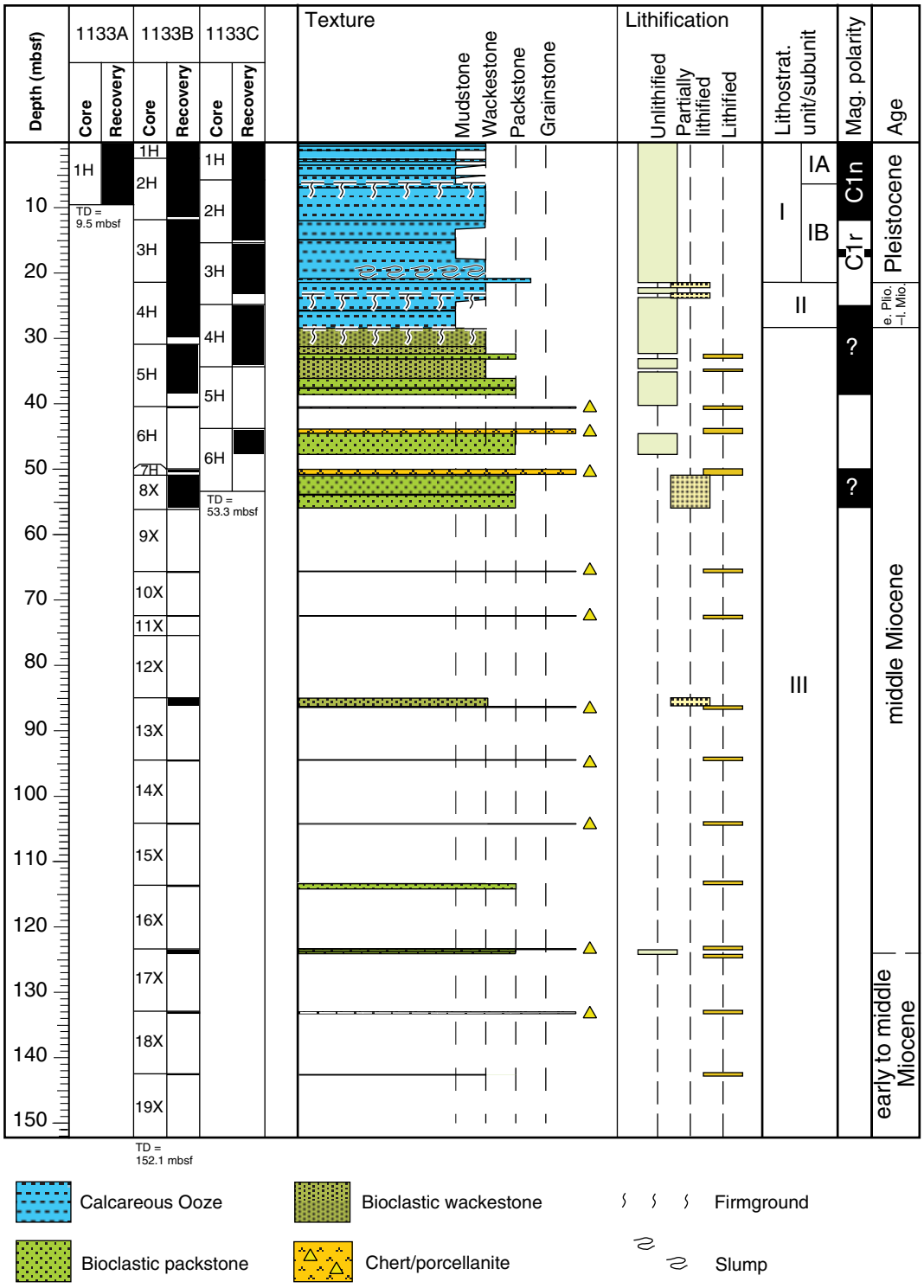

Figure F4. Boundary between Unit I and Unit II (interval 182-1133B-4H-1, 0–14 cm). Note the sharp scoured surface.

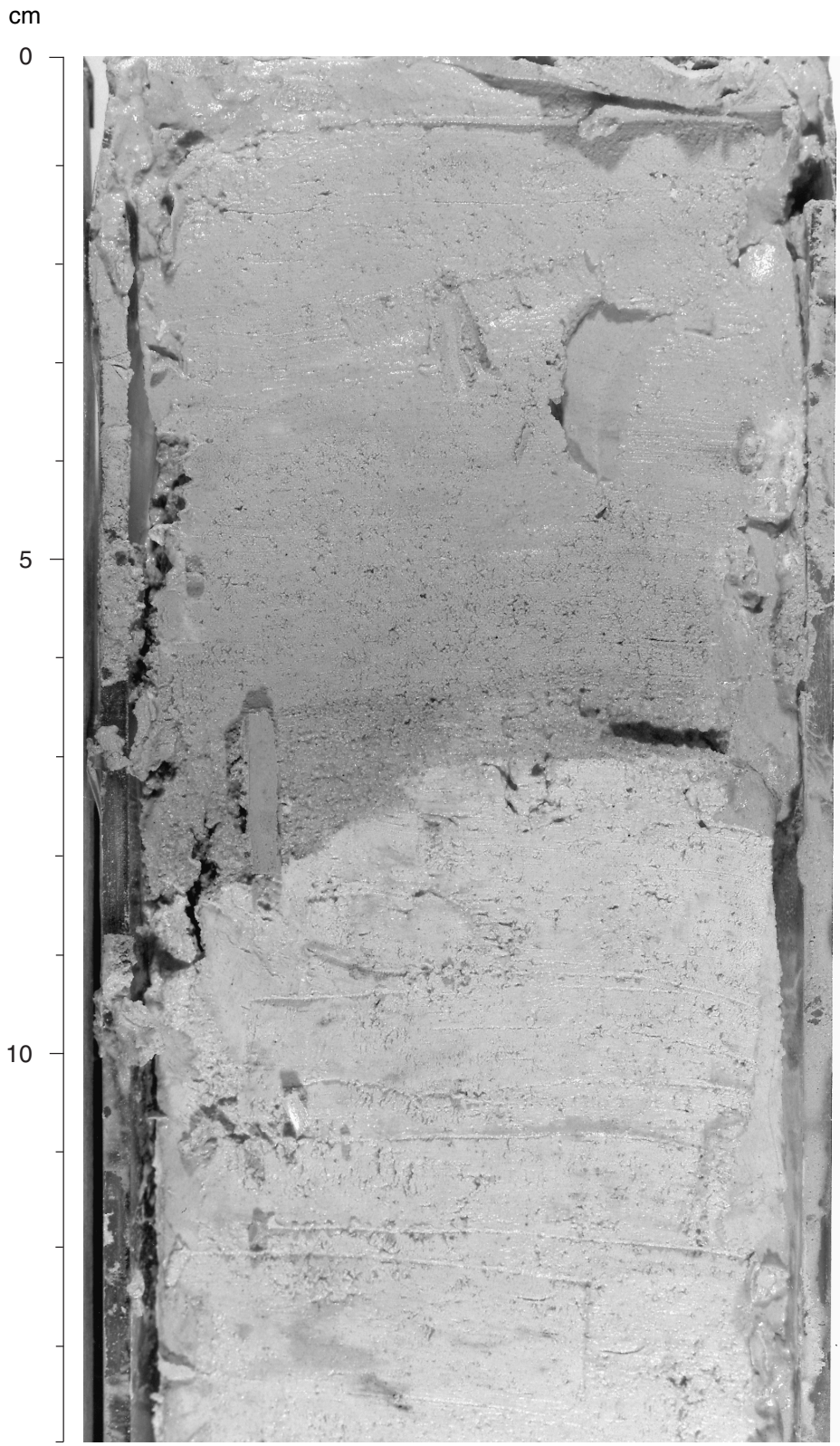

Figure F5. Inclined, deformed beds (interval 182-1133B-3H-6, 105–150 cm). The soft sediment deformation is interpreted to be a slump deposit.

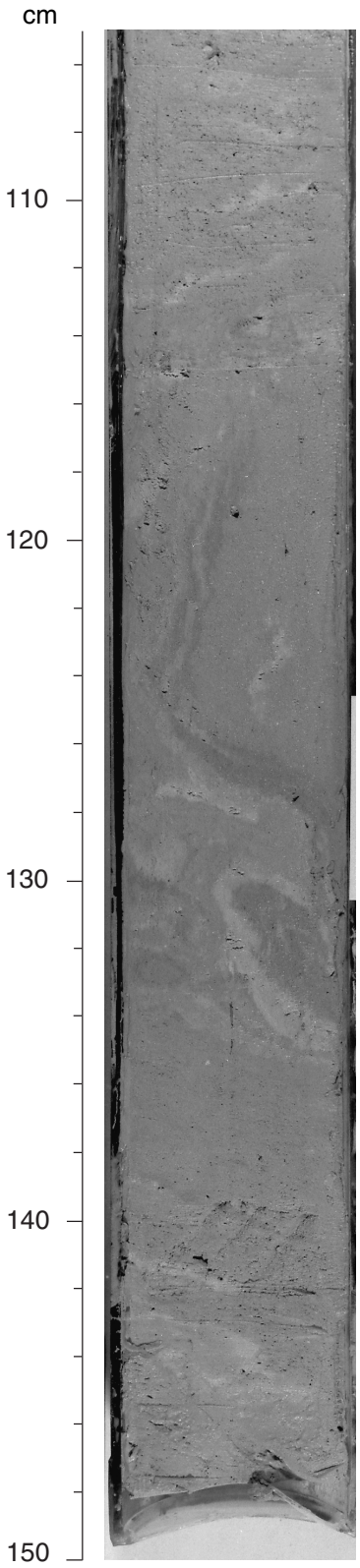

Figure F6. Stratigraphic position of calcareous nannofossil and planktonic foraminifer zones, with benthic foraminifer assemblages, Site 1133. Dashed boundaries imply uncertainty. No sample = the core catcher, if recovered, did not contain enough sediment to prepare for foraminifers.

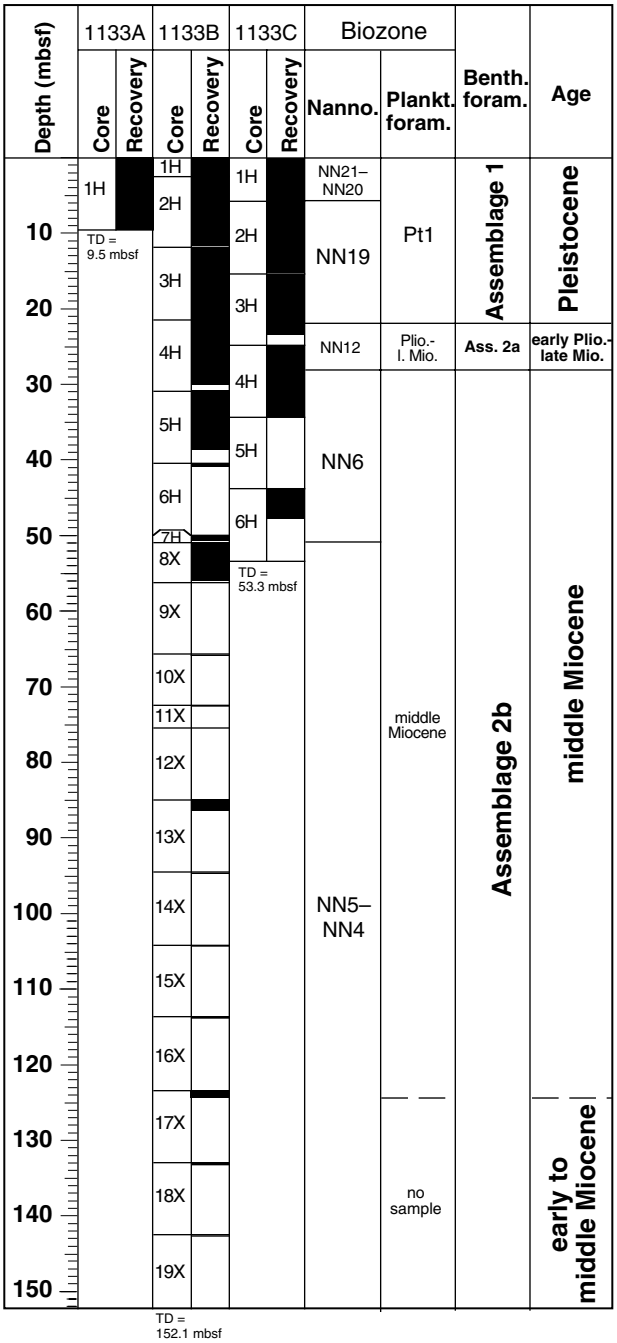

Figure F7. Sedimentation rate curve constructed from the datum levels for Site 1133 listed in Table T2, p. 37. Stratigraphic error varies between ±0.06 and ±5.43 m, as indicated by the length of error bars.

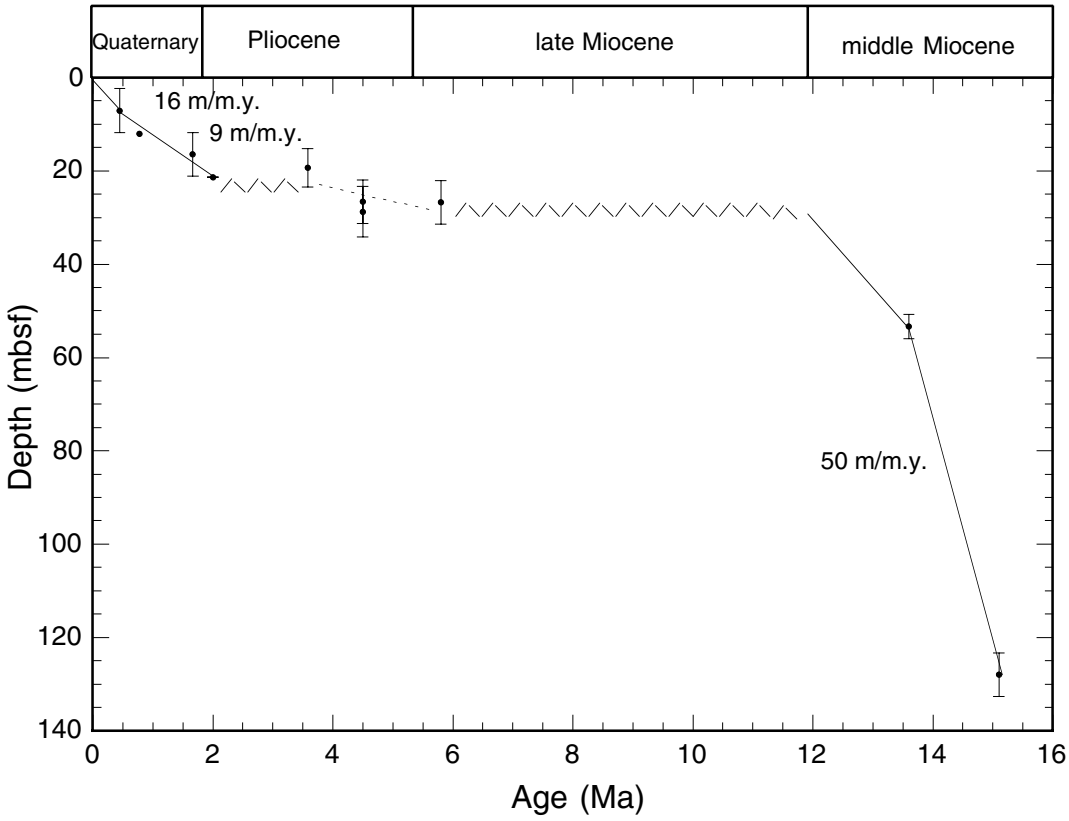

Figure F8. Downhole inclination of (**A**) Hole 1133B and **(B**) Hole 1133C, determined from natural remanent magnetization (NRM) long-core measurements and after partial demagnetization, together with interpreted magnetostratigraphy. Magnetic polarity is shown in the column to the right of each figure. Inclination data do not define a clear Gauss/Matuyama transition. This interval is indicated with a hash pattern in the magnetic polarity of (**A**).

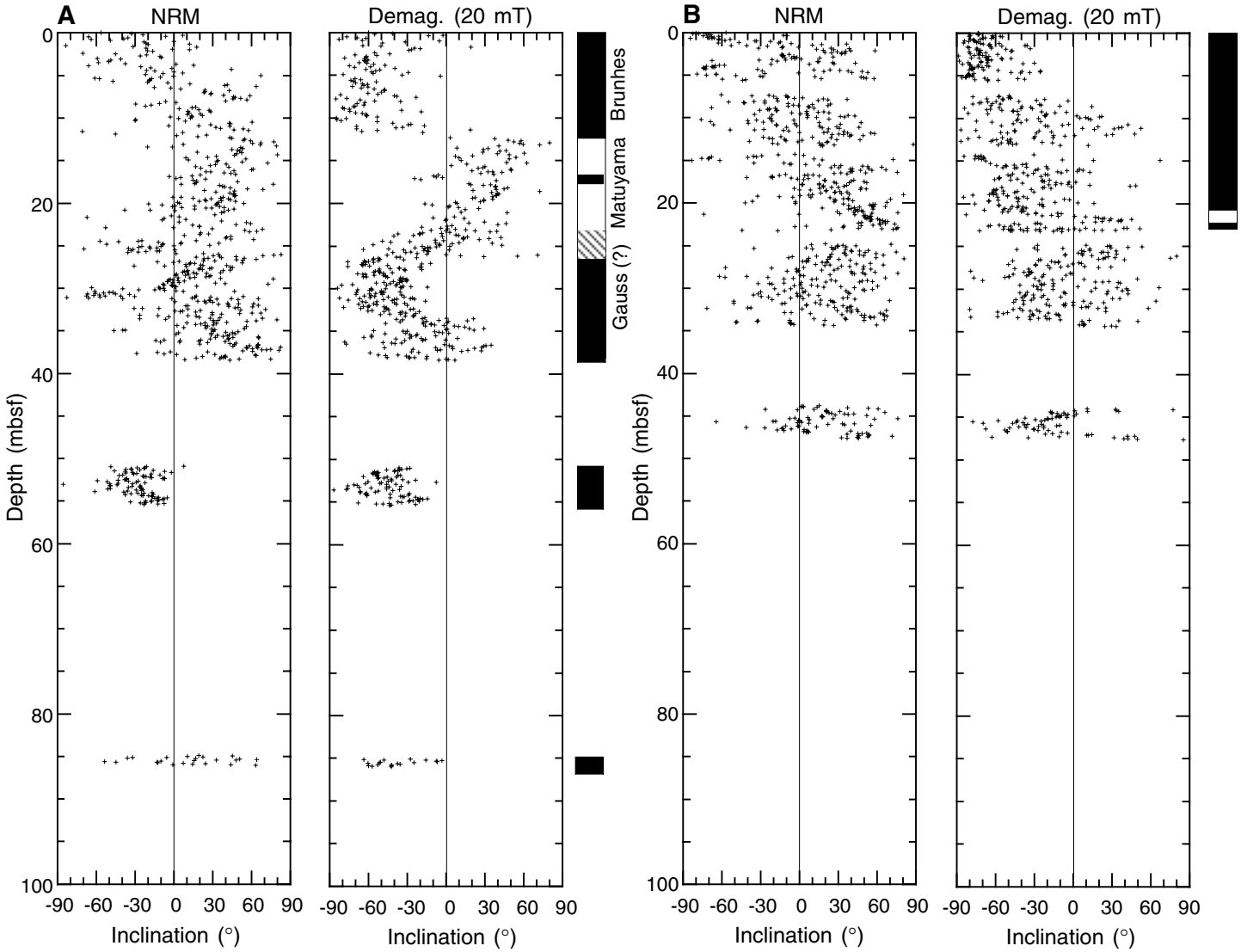

Figure F9. Demagnetization of natural remanent magnetization (NRM), anhysteretic remanent magnetization (ARM), and isothermal remanent magnetization (IRM), and of the acquisition of IRM (IRMA). The plot summarizes the magnetic characteristics of the samples. The IRM acquisition curves illustrated are consistent with the presence of magnetite. Demagnetization plots of NRM demonstrate that the samples are near the noise limit of the instrument. The ratios of ARM:IRM are indicative of larger contributions from multidomain magnetite. The high coercivity of the SIRM suggests that magnetic sulfides may be present as well.

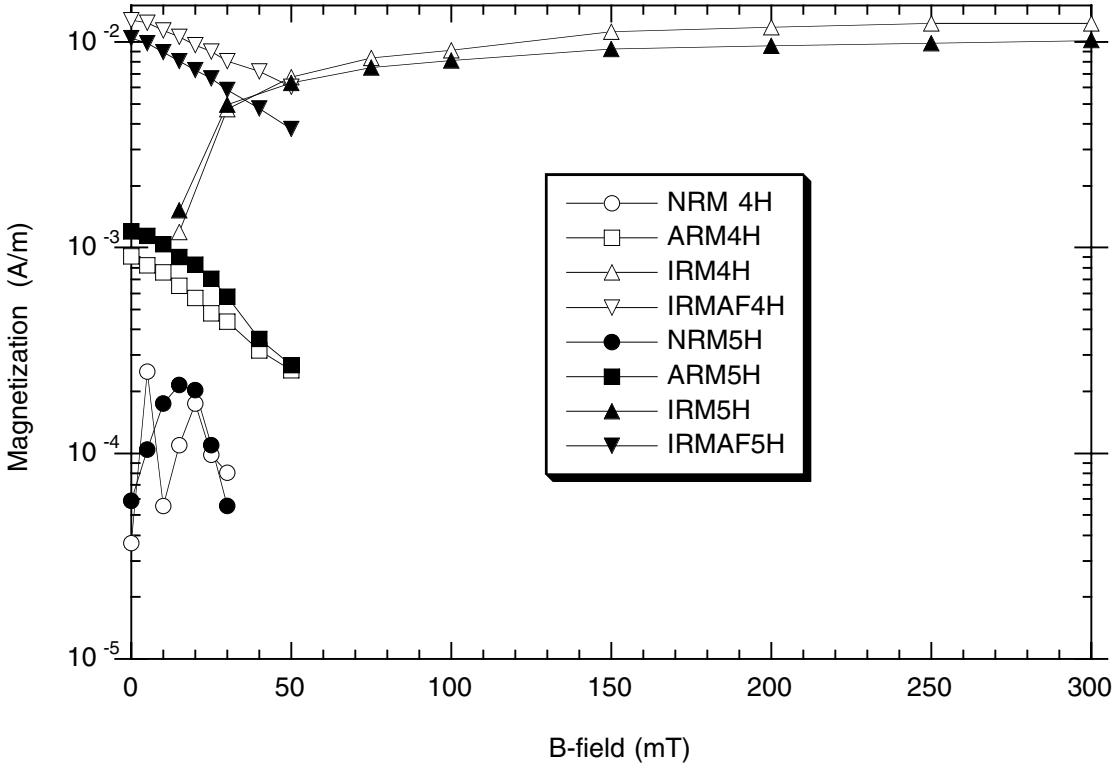

Figure F10. Composite depth section produced using the Splicer software. The black line represents data from Hole 1133B, and the red line represents data from Hole 1133C. Data from Hole 1133C are offset for ease of comparison. All depths use the meters composite depth (mcd) scale. For conversions from mcd to mbsf, see Table T3, p. 38.

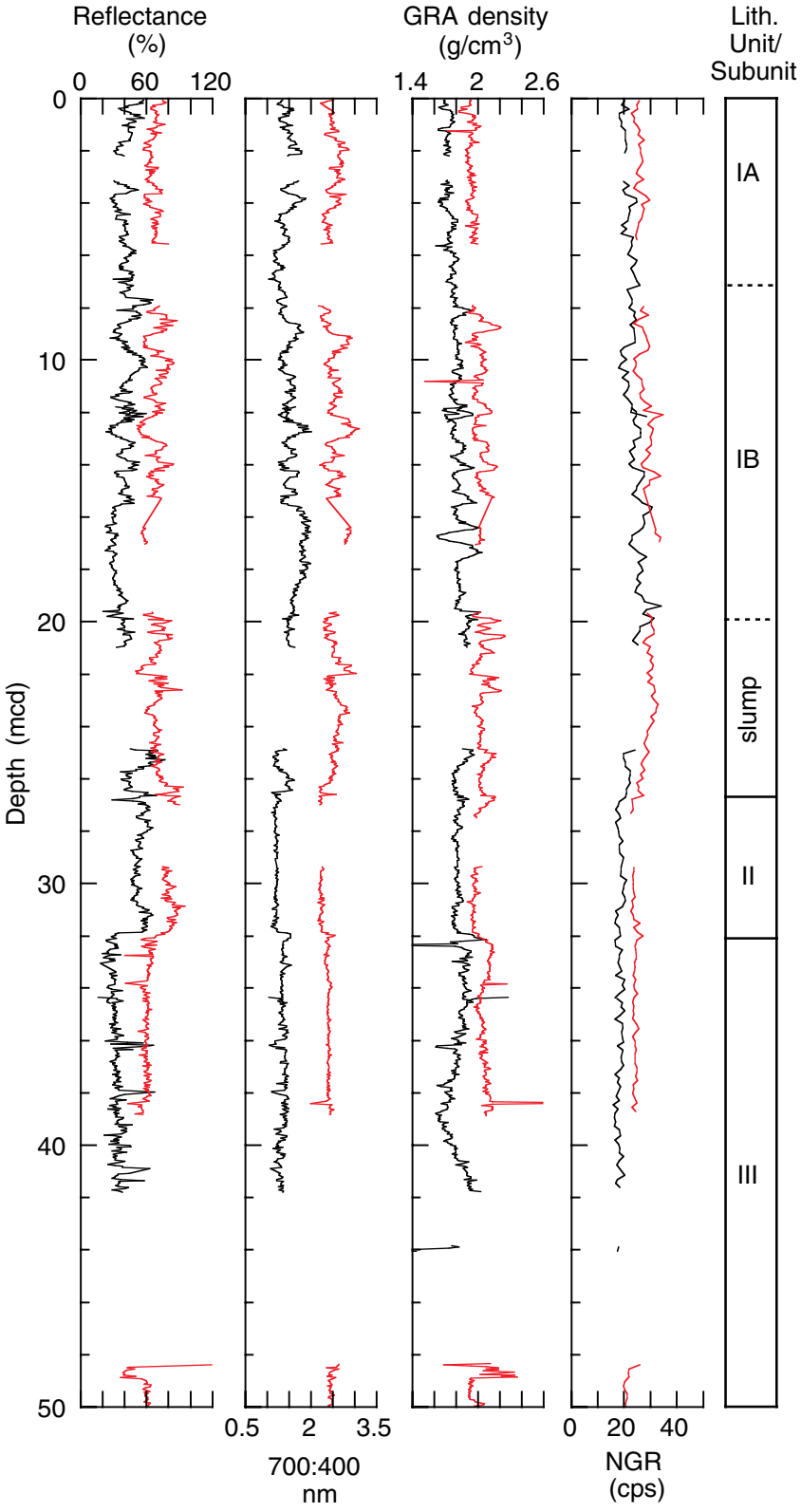

Figure F11. Spliced section of 400-nm color reflectance data, color reflectance ratio data (700:400 nm), gamma-ray attenuation (GRA) density data, and natural gamma radiation (NGR) data produced using the Splicer software. These data are a spliced composite of correlated data from Holes 1133B and 1133C. Ages are derived from biostratigraphic data (see **"Biostratigraphy,"** p. 7). Lithostratigraphic units are described in **"Lithostratigraphy,"** p. 3.

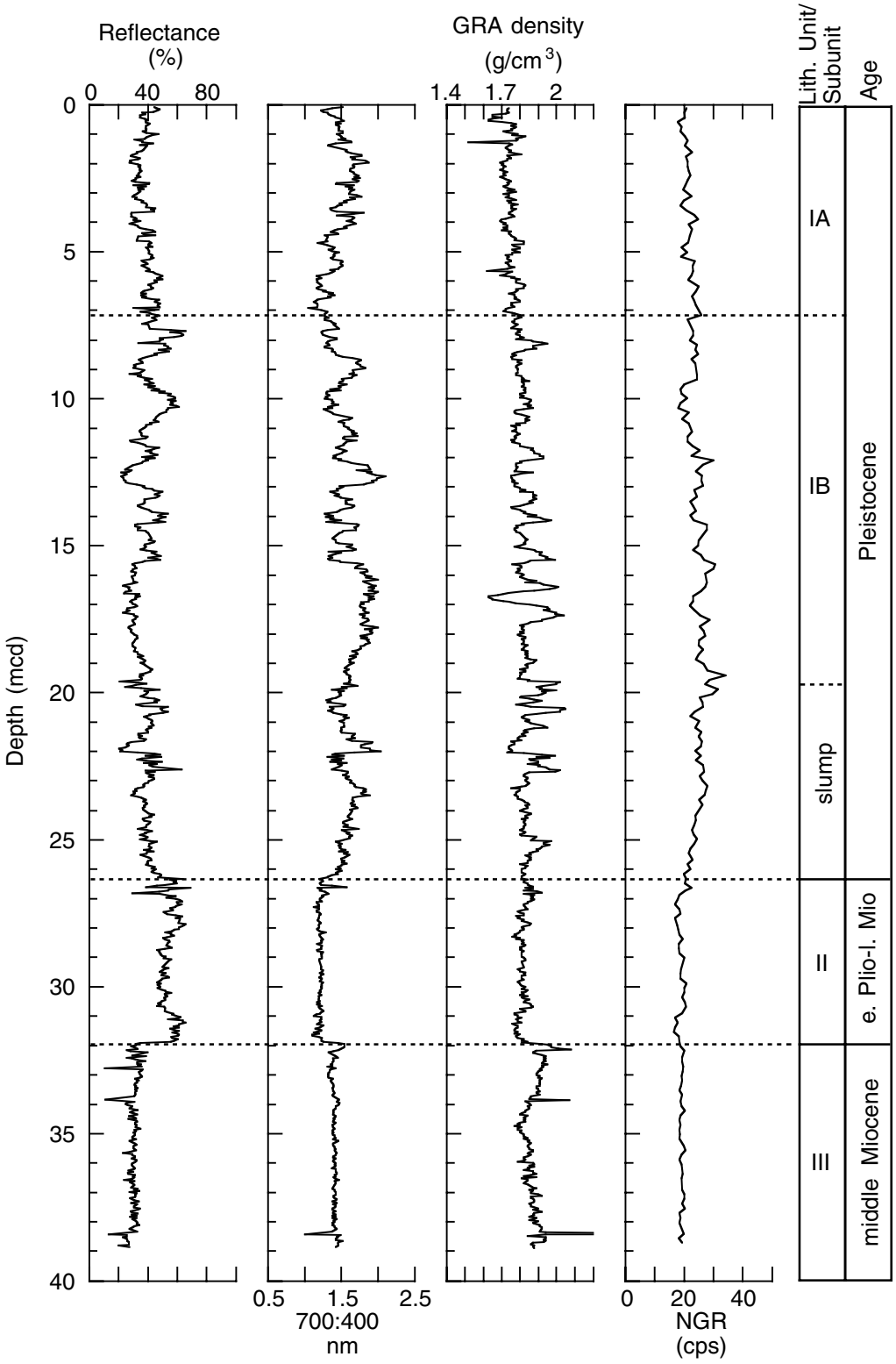

Figure F12. Calcium carbonate and organic carbon contents of samples from Site 1133. Solid circles = Hole 1133A; open circles = Hole 1133B.

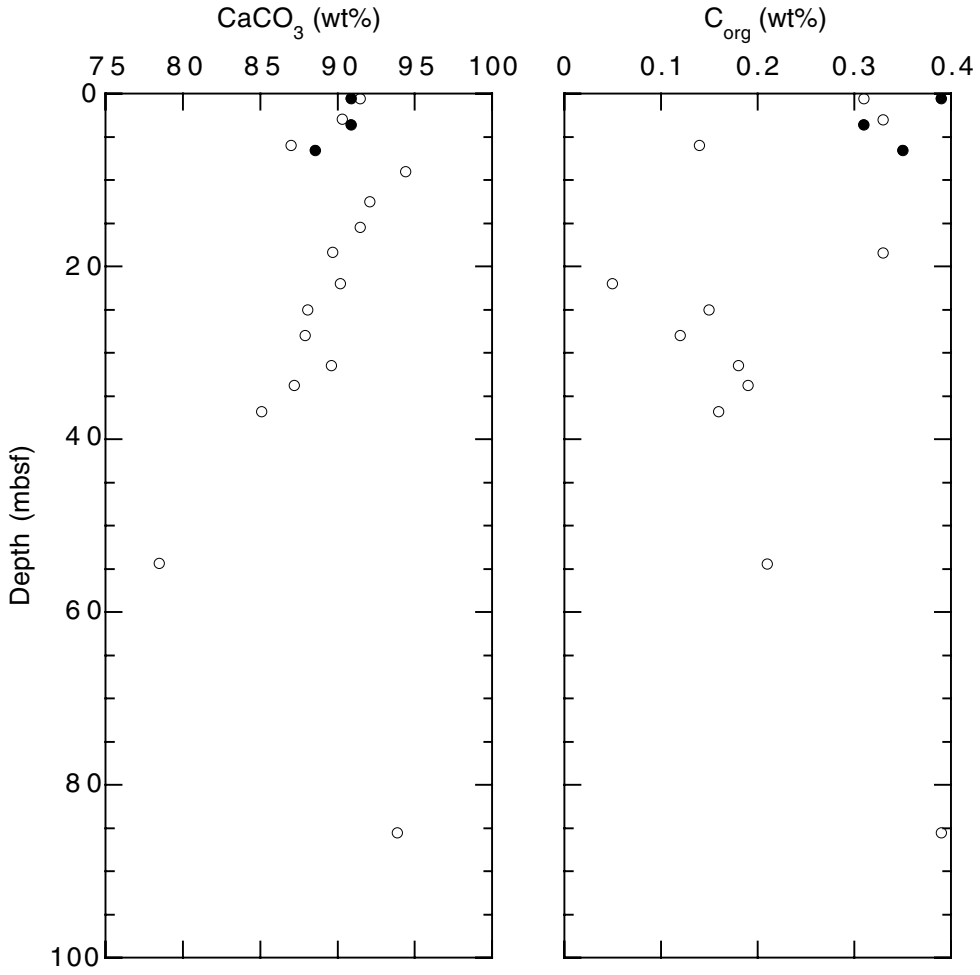

Figure F13. Depths vs. concentration profiles for (**A**) salinity, (**B**) Cl^-, (**C**) Ca^{2+}, (**D**) Mg^{2+}, (**E**) K^+, and (**F**) Sr^{2+}; Site 1133.

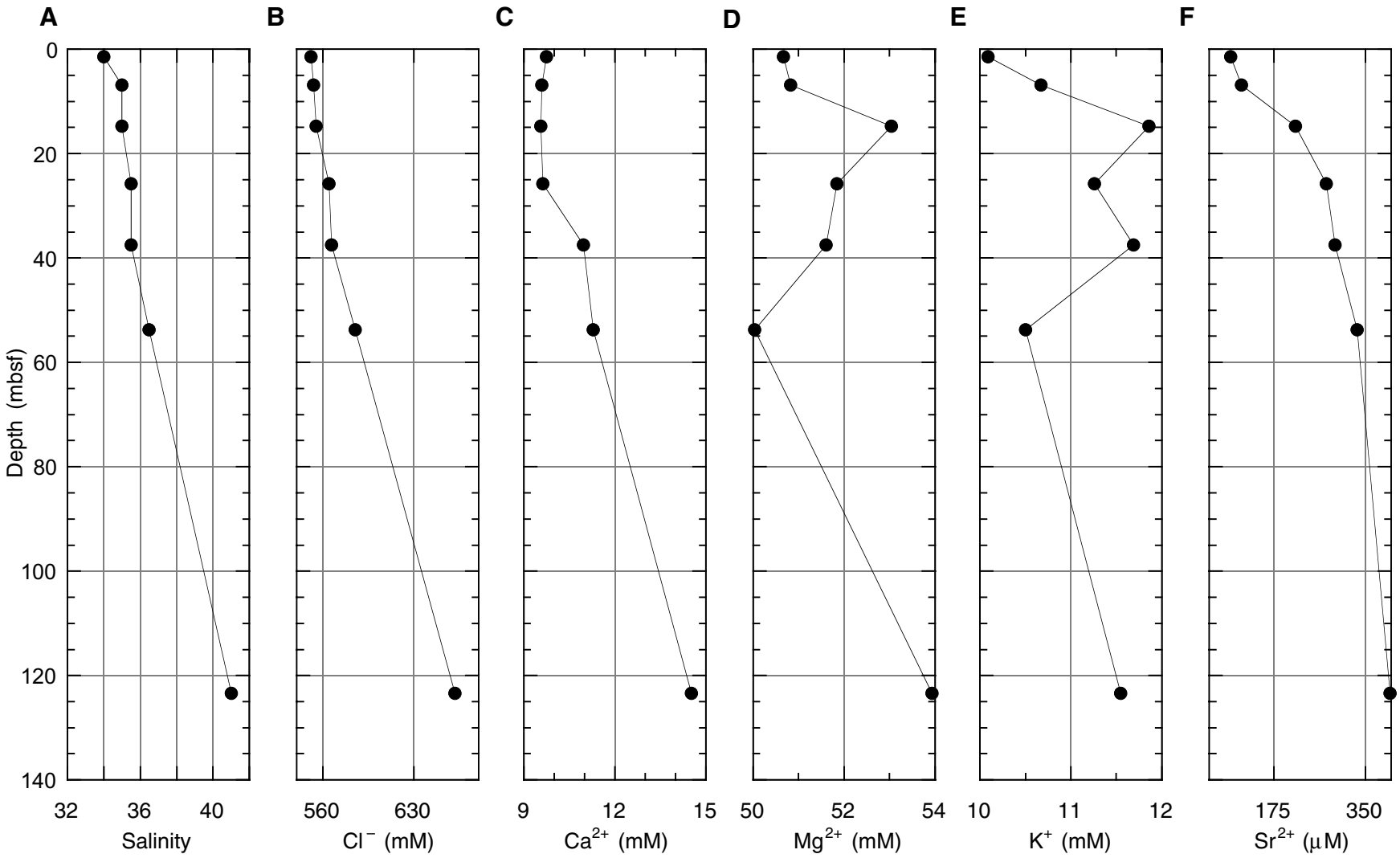

Figure F14. Depths vs. concentration profiles for (**A**) $H_4SiO_4^0$, (**B**) Li^+, (**C**) Fe^{2+}, (**D**) NH_4^+, (**E**) SO_4^{2-}, (**F**) pH, and (**G**) alkalinity.

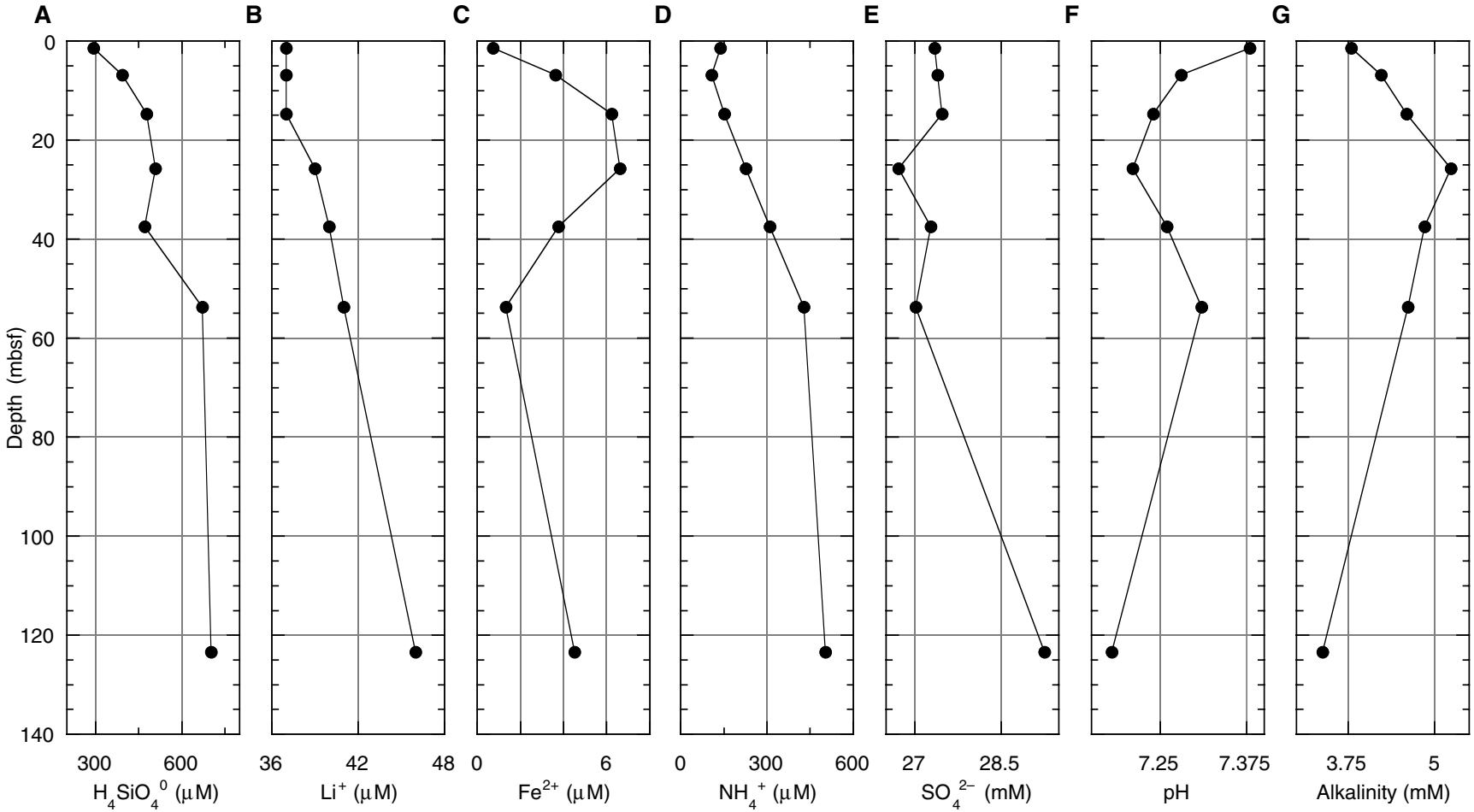

Figure F15. Combined plot of core recovery; natural gamma radiation (NGR); uncorrected gamma-ray attenuation (GRA; red line) and moisture-and-density (MAD; blue dots) bulk densities; *P*-wave velocity, after omitting high-velocity data measured in chert intervals to better visualize low-velocity variability; and porosity from Site 1133. Physical properties units (PP units), biostratigraphic ages, and lithostratigraphic units are indicated on the right.

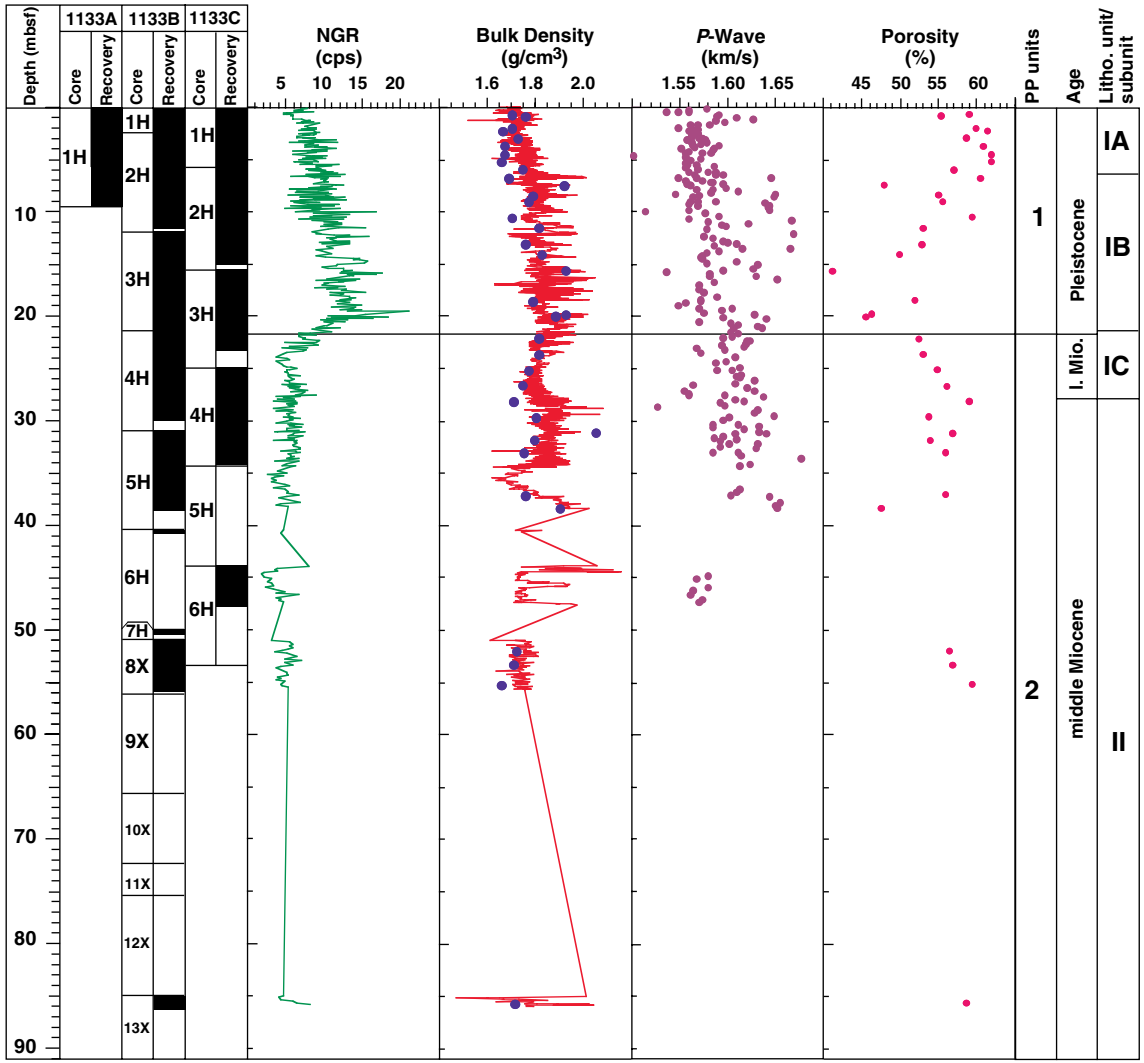

Figure F16. Shear strength data from Site 1133.

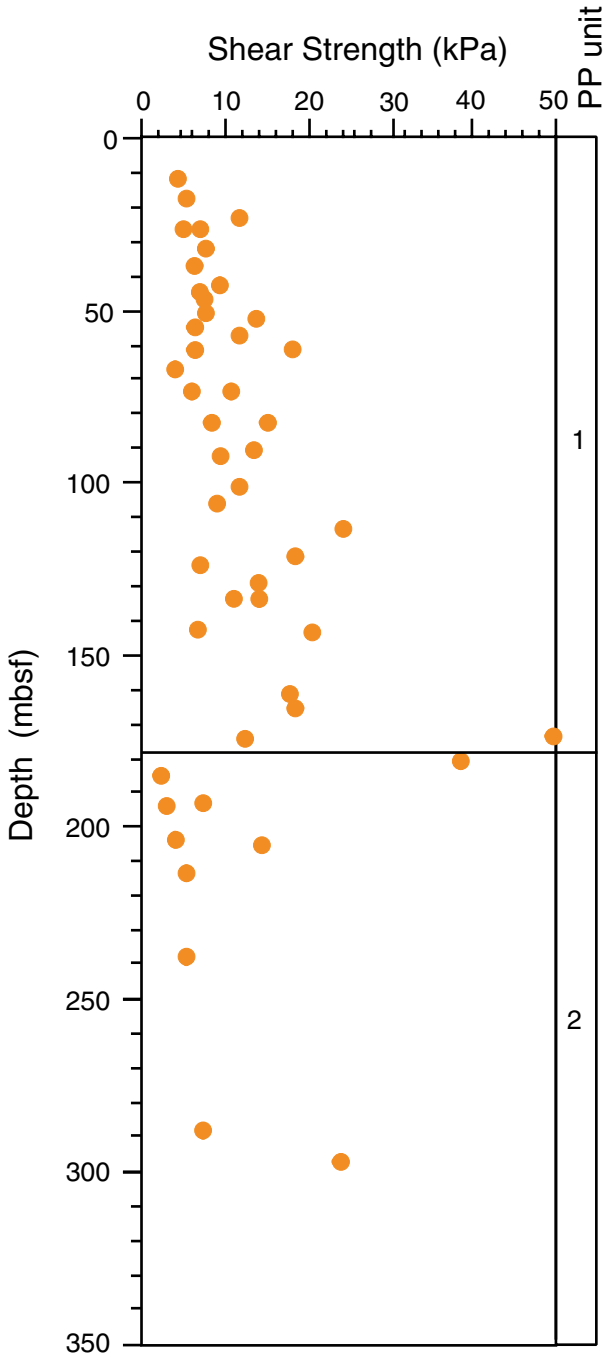

Figure F17. Thermal conductivity and bulk density data with PP units for Site 1133. GRA = gamma-ray attenuation.

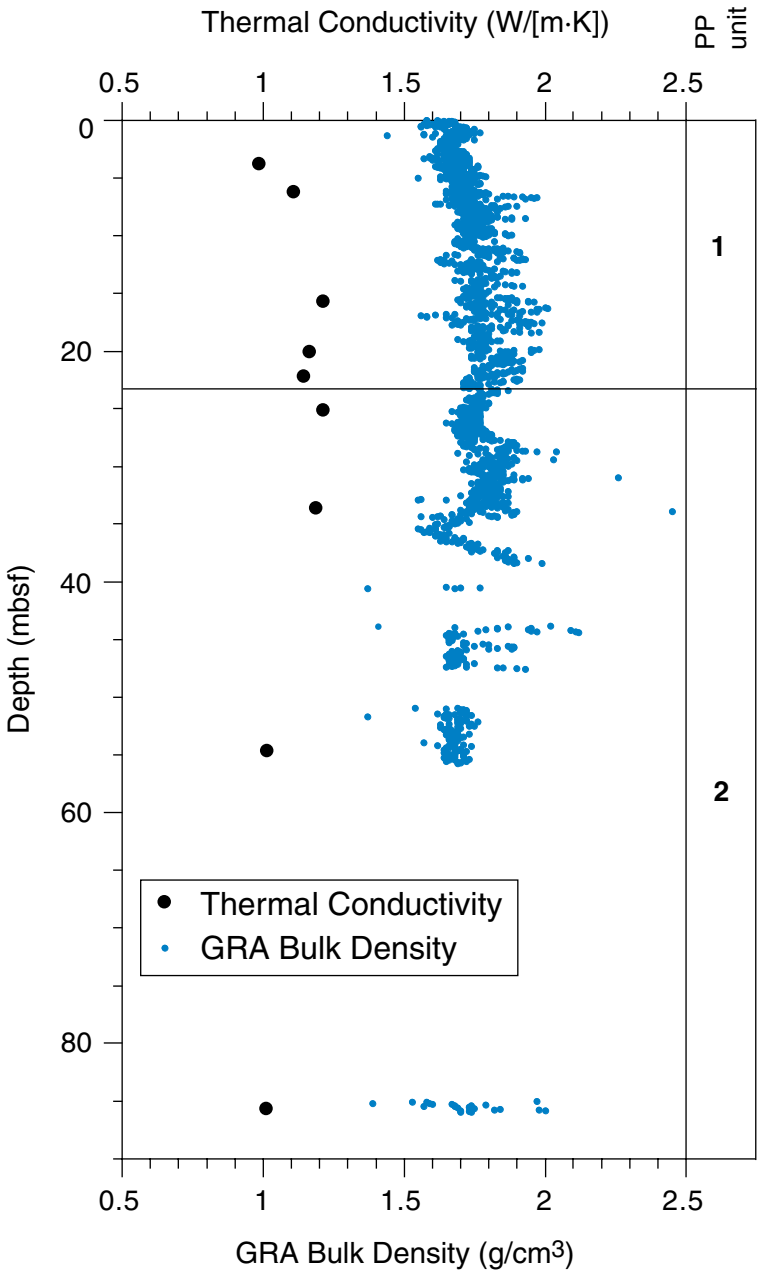

Table T1. Site 1133 coring summary. (See table note. Continued on next page.)

Hole 1133A

Latitude: –33.539490° (33°32.3694′S)
Longitude: 128.905100° (128°54.3060′E)
Seafloor (drill-pipe measurement from rig floor, mbrf): 1049.0
Distance between rig floor and sea level (m): 11.8
Water depth (drill-pipe measurement from sea level, m): 1037.2
Total depth (from rig floor, mbrf): 1058.5
Penetration (mbsf): 9.5
Total number of cores: 1
Total length of cored section (m): 9.5
Total core recovered (m): 9.78
Core recovery (%): 103.0

Hole 1133B

Latitude: –33.539640° (33°32.3784′S)
Longitude: 128.905290° (128°54.3174′E)
Seafloor (drill-pipe measurement from rig floor, mbrf): 1049.1
Distance between rig floor and sea level (m): 11.9
Water depth (drill-pipe measurement from sea level, m): 1037.2
Total depth (from rig floor, mbrf): 1201.2
Penetration (mbsf): 152.1
Total number of cores: 19
Total length of cored section (m): 152.1
Total core recovered (m): 48.59
Core recovery (%): 32.0

Hole 1133C

Latitude: –33.539810° (33°32.3886′S)
Longitude: 128.905350° (128°54.3210′E)
Seafloor (drill-pipe measurement from rig floor, mbrf): 1048.7
Distance between rig floor and sea level (m): 11.9
Water depth (drill-pipe measurement from sea level, m): 1036.8
Total depth (from rig floor, mbrf): 1102.0
Penetration (mbsf): 53.30
Total number of cores: 6
Total length of cored section (m): 53.3
Total core recovered (m): 37.26
Core recovery (%): 69.9

Core	Date (Nov 1998)	Time (UTC + 8 hr)	Depth (mbsf)	Length cored (m)	Length recovered (m)	Recovery (%)	Comment
182-1133A-							
1H	27	0225	0.00-9.50	9.5	9.78	103.0	
Totals:				9.5	9.78	103.0	
182-1133B-							
1H	27	0300	0.00-2.40	2.4	2.40	100.0	
2H	27	0340	2.40-11.90	9.5	9.43	99.3	
3H	27	0415	11.90-21.40	9.5	9.46	99.6	
4H	27	0525	21.40-30.90	9.5	9.99	105.2	
5H	27	0605	30.90-40.40	9.5	7.67	80.7	
6H	27	0700	40.40-49.90	9.5	0.29	3.1	
7H	27	0755	49.90-50.90	1.0	0.83	83.0	
8X	27	0900	50.90-56.10	5.2	5.04	96.9	
9X	27	0945	56.10-65.70	9.6	0.02	0.2	
10X	27	1055	65.70-72.30	6.6	0.12	1.8	
11X	27	1210	72.30-75.30	3.0	0.10	3.3	
12X	27	1300	75.30-84.90	9.6	0.01	0.1	All to PALEO
13X	27	1355	84.90-94.50	9.6	1.49	15.5	
14X	27	1430	94.50-104.10	9.6	0.12	1.3	
15X	27	1555	104.10-113.70	9.6	0.17	1.8	
16X	27	1655	113.70-123.30	9.6	0.19	2.0	
17X	27	1750	123.30-132.90	9.6	0.84	8.8	
18X	27	1850	132.90-142.50	9.6	0.33	3.4	
19X	27	1945	142.50-152.10	9.6	0.09	0.9	
Totals:				152.1	48.59	32.0	

Table T1 (continued).

Core	Date (Nov 1998)	Time (UTC + 8 hr)	Depth (mbsf)	Length cored (m)	Length recovered (m)	Recovery (%)	Comment
182-1133C-							
1H	27	2300	0.00-5.80	5.8	5.74	99.0	
2H	27	2355	5.80-15.30	9.5	9.39	98.8	
3H	28	0050	15.30-24.80	9.5	8.21	86.4	
4H	28	0150	24.80-34.30	9.5	9.83	103.5	
5H	28	0255	34.30-43.80	9.5	0.09	1.0	
6H	28	0355	43.80-53.30	9.5	4.00	42.1	
Totals:				53.3	37.26	69.9	

Note: UTC = Universal Time Coordinated, PALEO = Paleontology Laboratory.

Table T2. Datum levels used for the calculation of the Site 1133 sedimentation rate.

Datum type	Datum level	Age (Ma)	Midpoint (mbsf)	Stratigraphic error (m)	Fossil group	Upper sample		Lower sample	
						Core, section, interval (cm)	Depth (mbsf)	Core, section, interval (cm)	Depth (mbsf)
						182-1133B-		182-1133B-	
T	*P. lacunosa*	0.45	7.12	4.72	1	1H-CC, 12-15	2.37	2H-CC, 6-11.8	11.80
T	*C. macintyrei*	1.67	16.47	4.72	1	2H-CC, 6-9	2.37	3H-CC, 13-16	11.80
B	Brunhes/Matuyama	0.78	12			3H-1			
B	*G. truncatulinoides*	2	21.39	0.06	4	3H-CC, 13-16	21.33	4H-1, 4-6	21.44
B	*G. crassaformis*	4.5	26.69	4.67	4	4H-1, 62-64	22.02	4H-CC, 11-14	31.36
T	*G. dehiscens*	5.8	26.72	4.68	4	4H-1, 62-64	22.02	4H-CC, 11-14	31.36
T	*S. heteromorphus*	13.6	53.34	2.61	1	7H-CC, 12-13	50.72	8X-CC, 14-17	55.91
B	*Orbulina*	15.1	128.00	4.68	4	17X-CC, 53-57	123.83	18X-CC, 30-33	133.20
						182-1133C-		182-1133C-	
T	*G. margaritae*	3.58	19.35	4.16	4	2H-CC, 11-14	15.16	3H-CC, 20-23	23.48
B	*G. puncticulata*	4.5	28.91	5.43	4	3H-CC, 20-23	23.48	4H-CC, 17-20	34.6

Notes: T = top of taxon stratigraphic range, B = bottom of taxon stratigraphic range. Midpoint is the middle depth between the sample where the taxon occurs and the adjacent sample where it does not occur. Stratigraphic error is one-half the distance between the sample where the taxon occurs and the adjacent sample where it does not occur. Fossil groups = calcareous nannofossils (1) and planktonic foraminifers (4).

Table T3. Core and section depths in mcd and mbsf, Site 1133.

Leg	Site	Hole	Core	Type	Section	Depth (mbsf)	Offset (m)	Depth (mcd)
182	1133	B	1	H	1	0.00	0.00	0.00
182	1133	B	1	H	2	1.50	0.00	1.50
182	1133	B	2	H	1	2.40	0.68	3.08
182	1133	B	2	H	2	3.90	0.68	4.58
182	1133	B	2	H	3	5.40	0.68	6.08
182	1133	B	2	H	4	6.90	0.68	7.58
182	1133	B	2	H	5	8.40	0.68	9.08
182	1133	B	2	H	6	9.90	0.68	10.58
182	1133	B	2	H	7	10.90	0.68	11.58
182	1133	B	3	H	1	11.90	–0.18	11.72
182	1133	B	3	H	2	13.40	–0.18	13.22
182	1133	B	3	H	3	14.90	–0.18	14.72
182	1133	B	3	H	4	16.31	–0.18	16.13
182	1133	B	3	H	5	17.81	–0.18	17.63
182	1133	B	3	H	6	19.31	–0.18	19.13
182	1133	B	3	H	7	20.81	–0.18	20.63
182	1133	B	4	H	1	21.40	3.39	24.79
182	1133	B	4	H	2	22.90	3.39	26.29
182	1133	B	4	H	3	24.40	3.39	27.79
182	1133	B	4	H	4	25.90	3.39	29.29
182	1133	B	4	H	5	27.40	3.39	30.79
182	1133	B	4	H	6	28.90	3.39	32.29
182	1133	B	4	H	7	30.40	3.39	33.79
182	1133	B	5	H	1	30.90	3.39	34.29
182	1133	B	5	H	2	32.40	3.39	35.79
182	1133	B	5	H	3	33.15	3.39	36.54
182	1133	B	5	H	4	34.65	3.39	38.04
182	1133	B	5	H	5	36.15	3.39	39.54
182	1133	B	5	H	6	37.65	3.39	41.04
182	1133	B	6	H	1	40.40	3.39	43.79
182	1133	B	8	X	1	50.90	3.39	54.29
182	1133	B	8	X	2	52.40	3.39	55.79
182	1133	B	8	X	3	53.90	3.39	57.29
182	1133	B	8	X	4	55.40	3.39	58.79
182	1133	B	13	X	1	84.90	3.39	88.29
182	1133	C	1	H	1	0.00	0.00	0.00
182	1133	C	1	H	2	1.50	0.00	1.50
182	1133	C	1	H	3	3.00	0.00	3.00
182	1133	C	1	H	4	4.50	0.00	4.50
182	1133	C	2	H	1	5.80	2.06	7.86
182	1133	C	2	H	2	7.30	2.06	9.36
182	1133	C	2	H	3	8.80	2.06	10.86
182	1133	C	2	H	4	10.30	2.06	12.36
182	1133	C	2	H	5	11.80	2.06	13.86
182	1133	C	2	H	7	14.30	2.06	16.36
182	1133	C	3	H	1	15.30	4.27	19.57
182	1133	C	3	H	2	16.80	4.27	21.07
182	1133	C	3	H	3	18.30	4.27	22.57
182	1133	C	3	H	4	19.80	4.27	24.07
182	1133	C	3	H	5	21.30	4.27	25.57
182	1133	C	3	H	6	22.80	4.27	27.07
182	1133	C	4	H	1	24.80	4.49	29.29
182	1133	C	4	H	2	26.30	4.49	30.79
182	1133	C	4	H	3	27.80	4.49	32.29
182	1133	C	4	H	4	29.30	4.49	33.79
182	1133	C	4	H	5	30.80	4.49	35.29
182	1133	C	4	H	6	32.30	4.49	36.79
182	1133	C	4	H	7	33.80	4.49	38.29
182	1133	C	6	H	1	43.80	4.49	48.29
182	1133	C	6	H	2	45.30	4.49	49.79
182	1133	C	6	H	3	46.80	4.49	51.29

Notes: Depths measured at top of each section. This table is also available in **ASCII format.**

Table T4. Splice tie points, Site 1133.

Site	Hole	Core	Type	Section	Interval (cm)	Depth (mbsf)	Depth (mcd)		Site	Hole	Core	Type	Section	Interval (cm)	Depth (mbsf)	Depth (mcd)
1133	C	1	H	3	132	4.32	4.32	Tie to	1133	B	2	H	1	128	3.68	4.36
1133	B	2	H	6	40	10.30	10.98	Tie to	1133	C	2	H	3	16	8.96	11.02
1133	C	2	H	4	56	10.86	12.92	Tie to	1133	B	3	H	1	124	13.14	12.96
1133	B	3	H	6	96	20.27	20.09	Tie to	1133	C	3	H	1	56	15.86	20.13
1133	C	3	H	5	104	22.34	26.61	Tie to	1133	B	4	H	2	36	23.26	26.65
1133	B	4	H	5	136	28.76	32.15	Tie to	1133	C	4	H	2	140	27.70	32.19
1133	C	4	H	7	59	34.39	38.88	Tie to	1133							

Note: This table is also available in **ASCII format.**

Table T5. Composition of headspace gases, Hole 1133B.

Core, section, interval (cm)	Depth (mbsf)	C_1 (ppmv)
182-1133B-		
1H-2, 0-5	1.50	169
2H-4, 0-5	6.90	11
3H-3, 0-5	14.90	6
4H-4, 0-5	25.90	70
5H-6, 0-5	37.65	3
8X3, 0-5	53.90	8
13X1, 110-113	86.00	7
17X-CC, 8-10	123.38	7
18X-CC, 0-2	132.90	3

Note: Ethane was not detected.

Table T6. Calcium carbonate ($CaCO_3$), organic carbon (C_{org}), nitrogen (N), and sulfur (S) data, Site 1133.

Core, section, interval (cm)	Depth (mbsf)	$CaCO_3$ (wt%)	C_{org} (wt%)	N (wt%)	S (wt%)
182-1133A-					
1H-1, 60-61	0.60	90.9	0.39	0.08	0.22
1H-3, 60-61	3.60	90.9	0.31	0.06	0.36
1H-5, 60-61	6.60	88.6	0.35	0.05	0.34
182-1133B-					
1H-1, 60-61	0.60	91.5	0.31	0.20	0.30
2H-1, 60-61	3.00	90.3	0.33	0.07	0.25
2H-3, 60-61	6.00	87.0	0.14		0.16
2H-5, 60-61	9.00	94.4			0.16
3H-1, 60-61	12.50	92.1			0.12
3H-3, 60-61	15.50	91.5			
3H-5, 60-61	18.41	89.7	0.33	0.05	0.26
4H-1, 60-61	22.00	90.2	0.05		
4H-3, 60-61	25.00	88.1	0.15		
4H-5, 60-61	28.00	87.9	0.12		
5H-1, 60-61	31.50	89.6	0.18		
5H-3, 60-61	33.75	87.2	0.19		0.09
5H-5, 60-61	36.75	85.1	0.16		
8X-3, 51-51	54.41	78.5	0.21		
13X-1, 59-60	85.49	93.9	0.39		0.05

Note: Blank = not detected.

Table T7. Interstitial water geochemistry, Site 1133.

Core, section, interval (cm)	Depth (mbsf)	pH	ppH	Alkalinity (mM)	Salinity	Cl^- (mM)	SO_4^{2-} (mM)	Na^+ (mM)	K^+ (mM)	Mg^{2+} (mM)	Ca^{2+} (mM)	Sr^{2+} (µM)	Li^+ (µM)	$H_4SiO_4^0$ (µM)	NH_4^+ (µM)	Fe^{2+} (µM)
182-1133B-																
1H-1, 145-150	1.45	7.38	7.45	3.80	34.0	551	27.4	468	9.4	53.4	10.1	91	37	294	138	0.7
2H-3, 145-150	6.85	7.28	7.47	4.23	35.0	553	27.4	469	10.0	53.6	10.0	112	37	393	109	3.6
3H-2, 140-150	14.80	7.24	7.33	4.60	35.0	555	27.5	470	11.1	55.9	9.9	216	37	478	153	6.2
4H-3, 140-150	25.80	7.21	7.24	5.24	35.5	565	26.7	480	10.5	54.6	10.0	275	39	509	228	6.6
5H-5, 140-150	37.55	7.26	7.19	4.86	35.5	567	27.3	480	10.9	54.4	11.4	292	40	471	311	3.8
8X-2, 140-150	53.80	7.31	7.45	4.62	36.5	585	27.0	494	9.8	52.7	11.7	335	41	671	429	1.3
17X-CC, 10-20	123.40	7.18		3.38	41.0	662	29.3	565	10.8	56.8	15.1	398	46	702	503	4.5

Table T8. Summary of X-ray diffraction analysis, Site 1133.

Leg	Site	Hole	Core	Type	Section	Top (cm)	Bottom (cm)	Depth (mbsf)	Aragonite (wt%)	Quartz (wt%)	LMC (wt%)	HMC (wt%)	Dolomite (wt%)
182	1133	A	1	H	1	60	61	0.60	17	1	33	49	0
182	1133	A	1	H	3	60	61	3.60	15	1	26	59	0
182	1133	A	1	H	5	60	61	6.60	20	1	36	42	1
182	1133	B	1	H	1	60	61	0.60	17	0	33	48	2
182	1133	B	2	H	1	60	61	3.00	17	1	46	35	1
182	1133	B	2	H	3	60	61	6.00	19	1	51	28	0
182	1133	B	2	H	5	60	61	9.00	6	0	41	52	1
182	1133	B	3	H	1	60	61	12.50	16	1	71	11	1
182	1133	B	3	H	3	60	61	15.50	17	2	59	21	1
182	1133	B	3	H	5	60	61	18.41	21	1	53	23	1
182	1133	B	4	H	1	60	61	22.00	4	1	94	0	1
182	1133	B	4	H	3	60	61	25.00	0	1	99	0	0
182	1133	B	4	H	5	60	61	28.00	0	1	98	0	1
182	1133	B	5	H	1	60	61	31.50	3	2	93	0	2
182	1133	B	5	H	3	60	61	33.75	2	1	94	0	3
182	1133	B	5	H	5	60	61	36.75	2	2	93	0	3
182	1133	B	8	X	3	51	51	54.41	4	1	83	0	13
182	1133	B	13	X	1	59	60	85.49	4	0	95	0	2

Notes: LMC = low-Mg calcite, HMC = high-Mg calcite. This table is also available in **ASCII format.**

Table T9. *P*-wave velocity measurements from the multisensor track, Site 1133.

Leg	Site	Hole	Core	Type	Section	Interval (cm)	Depth (mbsf)	*Vp* (km/s)
182	1133	A	1	H	1	19.0	0.19	2.3041
182	1133	A	1	H	1	27.0	0.27	2.2981
182	1133	A	1	H	1	27.0	0.27	2.3866
182	1133	A	1	H	1	31.0	0.31	2.1537
182	1133	A	1	H	1	35.0	0.35	2.3014
182	1133	A	1	H	1	39.0	0.39	2.5191
182	1133	A	1	H	1	43.0	0.43	1.8197
182	1133	A	1	H	1	43.0	0.43	2.3071
182	1133	A	1	H	1	47.0	0.47	2.5803
182	1133	A	1	H	1	55.0	0.55	2.2955
182	1133	A	1	H	1	59.0	0.59	1.5290
182	1133	A	1	H	1	63.0	0.63	2.0289
182	1133	A	1	H	1	67.0	0.67	1.7519
182	1133	A	1	H	1	67.0	0.67	2.2948
182	1133	A	1	H	1	71.0	0.71	2.2988
182	1133	A	1	H	1	75.0	0.75	1.1203
182	1133	A	1	H	1	75.0	0.75	1.4880
182	1133	A	1	H	1	79.0	0.79	1.4338
182	1133	A	1	H	1	79.0	0.79	1.5059
182	1133	A	1	H	1	83.0	0.83	1.6407
182	1133	A	1	H	1	87.0	0.87	1.5076
182	1133	A	1	H	1	103.0	1.03	1.8234
182	1133	A	1	H	1	103.0	1.03	2.8760
182	1133	A	1	H	1	111.0	1.11	2.4830
182	1133	A	1	H	1	111.0	1.11	2.7444
182	1133	A	1	H	1	115.0	1.15	2.0823
182	1133	A	1	H	1	119.0	1.19	2.2584
182	1133	A	1	H	1	123.0	1.23	2.0517
182	1133	A	1	H	1	127.0	1.27	2.1227
182	1133	A	1	H	1	131.0	1.31	1.9483
182	1133	A	1	H	1	135.0	1.35	2.2143
182	1133	A	1	H	1	139.0	1.39	1.9260
182	1133	A	1	H	1	143.0	1.43	2.0633
182	1133	A	1	H	2	15.0	1.65	1.8496
182	1133	A	1	H	2	23.0	1.73	1.6677
182	1133	A	1	H	2	27.0	1.77	2.2896
182	1133	A	1	H	2	31.0	1.81	1.9346
182	1133	A	1	H	2	35.0	1.85	2.5832
182	1133	A	1	H	2	39.0	1.89	2.1086
182	1133	A	1	H	2	43.0	1.93	2.0780
182	1133	A	1	H	2	47.0	1.97	1.9617
182	1133	A	1	H	2	51.0	2.01	1.9043
182	1133	A	1	H	2	55.0	2.05	2.1446
182	1133	A	1	H	2	59.0	2.09	1.6012
182	1133	A	1	H	2	63.0	2.13	1.5447
182	1133	A	1	H	2	67.0	2.17	1.9541
182	1133	A	1	H	2	71.0	2.21	1.5512
182	1133	A	1	H	2	75.0	2.25	1.5012
182	1133	A	1	H	2	79.0	2.29	1.5009
182	1133	A	1	H	2	83.0	2.33	1.8796
182	1133	A	1	H	2	87.0	2.37	2.0334
182	1133	A	1	H	2	91.0	2.41	2.2683
182	1133	A	1	H	2	95.0	2.45	2.0648
182	1133	A	1	H	2	99.0	2.49	2.1416
182	1133	A	1	H	2	103.0	2.53	2.0588
182	1133	A	1	H	2	111.0	2.61	2.5765
182	1133	A	1	H	2	115.0	2.65	2.0269
182	1133	A	1	H	2	119.0	2.69	1.9676
182	1133	A	1	H	2	123.0	2.73	1.8468
182	1133	A	1	H	2	127.0	2.77	1.7708
182	1133	A	1	H	2	131.0	2.81	2.2475
182	1133	A	1	H	2	135.0	2.85	2.5027
182	1133	A	1	H	2	139.0	2.89	2.0059
182	1133	A	1	H	2	143.0	2.93	1.9717
182	1133	A	1	H	3	15.0	3.15	2.2989

Note: Only a portion of this table appears here. The complete table is available in **ASCII format.**

Table T10. Gamma-ray attenuation densiometry measurements from the multisensor track, Site 1133.

Leg	Site	Hole	Core	Type	Section	Interval (cm)	Depth (mbsf)	Density (g/cm^3)	Corrected density (g/cm^3)
182	1133	A	1	H	1	3.0	0.03	1.68	1.62
182	1133	A	1	H	1	7.0	0.07	1.74	1.67
182	1133	A	1	H	1	11.0	0.11	1.70	1.63
182	1133	A	1	H	1	15.0	0.15	1.73	1.67
182	1133	A	1	H	1	19.0	0.19	1.74	1.68
182	1133	A	1	H	1	23.0	0.23	1.71	1.65
182	1133	A	1	H	1	27.0	0.27	1.64	1.57
182	1133	A	1	H	1	31.0	0.31	1.67	1.60
182	1133	A	1	H	1	35.0	0.35	1.65	1.58
182	1133	A	1	H	1	39.0	0.39	1.69	1.62
182	1133	A	1	H	1	43.0	0.43	1.71	1.65
182	1133	A	1	H	1	47.0	0.47	1.75	1.68
182	1133	A	1	H	1	51.0	0.51	1.70	1.63
182	1133	A	1	H	1	55.0	0.55	1.67	1.61
182	1133	A	1	H	1	59.0	0.59	1.76	1.70
182	1133	A	1	H	1	63.0	0.63	1.77	1.71
182	1133	A	1	H	1	67.0	0.67	1.75	1.69
182	1133	A	1	H	1	71.0	0.71	1.71	1.64
182	1133	A	1	H	1	75.0	0.75	1.81	1.75
182	1133	A	1	H	1	79.0	0.79	1.77	1.71
182	1133	A	1	H	1	83.0	0.83	1.76	1.69
182	1133	A	1	H	1	87.0	0.87	1.76	1.70
182	1133	A	1	H	1	91.0	0.91	1.74	1.68
182	1133	A	1	H	1	95.0	0.95	1.78	1.72
182	1133	A	1	H	1	99.0	0.99	1.75	1.69
182	1133	A	1	H	1	103.0	1.03	1.77	1.71
182	1133	A	1	H	1	107.0	1.07	1.79	1.73
182	1133	A	1	H	1	111.0	1.11	1.77	1.70
182	1133	A	1	H	1	115.0	1.15	1.76	1.70
182	1133	A	1	H	1	119.0	1.19	1.77	1.71
182	1133	A	1	H	1	123.0	1.23	1.79	1.73
182	1133	A	1	H	1	127.0	1.27	1.78	1.72
182	1133	A	1	H	1	131.0	1.31	1.78	1.72
182	1133	A	1	H	1	135.0	1.35	1.76	1.70
182	1133	A	1	H	1	139.0	1.39	1.71	1.65
182	1133	A	1	H	1	143.0	1.43	1.67	1.60
182	1133	A	1	H	2	3.0	1.53	1.72	1.66
182	1133	A	1	H	2	7.0	1.57	1.78	1.72
182	1133	A	1	H	2	11.0	1.61	1.76	1.70
182	1133	A	1	H	2	15.0	1.65	1.75	1.69
182	1133	A	1	H	2	19.0	1.69	1.74	1.68
182	1133	A	1	H	2	23.0	1.73	1.75	1.68
182	1133	A	1	H	2	27.0	1.77	1.74	1.68
182	1133	A	1	H	2	31.0	1.81	1.71	1.65
182	1133	A	1	H	2	35.0	1.85	1.73	1.67
182	1133	A	1	H	2	39.0	1.89	1.74	1.67
182	1133	A	1	H	2	43.0	1.93	1.74	1.68
182	1133	A	1	H	2	47.0	1.97	1.75	1.69
182	1133	A	1	H	2	51.0	2.01	1.73	1.67
182	1133	A	1	H	2	55.0	2.05	1.72	1.65
182	1133	A	1	H	2	59.0	2.09	1.70	1.63
182	1133	A	1	H	2	63.0	2.13	1.74	1.68
182	1133	A	1	H	2	67.0	2.17	1.71	1.64
182	1133	A	1	H	2	71.0	2.21	1.74	1.67
182	1133	A	1	H	2	75.0	2.25	1.74	1.67
182	1133	A	1	H	2	79.0	2.29	1.73	1.67
182	1133	A	1	H	2	83.0	2.33	1.73	1.66
182	1133	A	1	H	2	87.0	2.37	1.73	1.67
182	1133	A	1	H	2	91.0	2.41	1.72	1.66
182	1133	A	1	H	2	95.0	2.45	1.73	1.66
182	1133	A	1	H	2	99.0	2.49	1.73	1.67
182	1133	A	1	H	2	103.0	2.53	1.73	1.67
182	1133	A	1	H	2	107.0	2.57	1.69	1.62
182	1133	A	1	H	2	111.0	2.61	1.72	1.66

Note: Only a portion of this table appears here. The complete table is available in **ASCII format.**

Table T11. Magnetic susceptibility measurements from the multisensor track, Site 1133.

Leg	Site	Hole	Core	Type	Section	Interval (cm)	Depth (mbsf)	Magnetic susceptibility (10^{-6}; SI units)	Corrected susceptibility (10^{-6}; SI units)
182	1133	A	1	H	1	3.0	0.03	3.8	3.8
182	1133	A	1	H	1	11.0	0.11	3.4	3.4
182	1133	A	1	H	1	19.0	0.19	5.6	5.6
182	1133	A	1	H	1	27.0	0.27	0.1	0.1
182	1133	A	1	H	1	35.0	0.35	–0.8	–0.8
182	1133	A	1	H	1	43.0	0.43	–1.2	–1.2
182	1133	A	1	H	1	51.0	0.51	–1.6	–1.6
182	1133	A	1	H	1	59.0	0.59	–1.4	–1.4
182	1133	A	1	H	1	67.0	0.67	–1.5	–1.5
182	1133	A	1	H	1	75.0	0.75	–1.7	–1.7
182	1133	A	1	H	1	83.0	0.83	–1.8	–1.8
182	1133	A	1	H	1	91.0	0.91	–1.6	–1.6
182	1133	A	1	H	1	99.0	0.99	–1.2	–1.2
182	1133	A	1	H	1	107.0	1.07	–1.5	–1.5
182	1133	A	1	H	1	115.0	1.15	–1.5	–1.5
182	1133	A	1	H	1	123.0	1.23	–1.8	–1.8
182	1133	A	1	H	1	131.0	1.31	–1.7	–1.7
182	1133	A	1	H	1	139.0	1.39	–1.7	–1.7
182	1133	A	1	H	1	147.0	1.47	–1.1	–1.1
182	1133	A	1	H	2	3.0	1.53	–2.8	–2.8
182	1133	A	1	H	2	11.0	1.61	–3.1	–3.1
182	1133	A	1	H	2	19.0	1.69	–2.8	–2.8
182	1133	A	1	H	2	27.0	1.77	–3.2	–3.2
182	1133	A	1	H	2	35.0	1.85	–3.0	–3.0
182	1133	A	1	H	2	43.0	1.93	–3.2	–3.2
182	1133	A	1	H	2	51.0	2.01	–3.4	–3.4
182	1133	A	1	H	2	59.0	2.09	–3.6	–3.6
182	1133	A	1	H	2	67.0	2.17	–2.8	–2.8
182	1133	A	1	H	2	75.0	2.25	–3.0	–3.0
182	1133	A	1	H	2	83.0	2.33	–3.2	–3.2
182	1133	A	1	H	2	91.0	2.41	–3.0	–3.0
182	1133	A	1	H	2	99.0	2.49	–2.8	–2.8
182	1133	A	1	H	2	107.0	2.57	–2.9	–2.9
182	1133	A	1	H	2	115.0	2.65	–3.1	–3.1
182	1133	A	1	H	2	123.0	2.73	–3.7	–3.7
182	1133	A	1	H	2	131.0	2.81	–3.1	–3.1
182	1133	A	1	H	2	139.0	2.89	–3.3	–3.3
182	1133	A	1	H	2	147.0	2.97	–3.0	–3.0
182	1133	A	1	H	3	3.0	3.03	–0.9	–0.9
182	1133	A	1	H	3	11.0	3.11	–0.9	–0.9
182	1133	A	1	H	3	19.0	3.19	–0.7	–0.7
182	1133	A	1	H	3	27.0	3.27	–0.8	–0.8
182	1133	A	1	H	3	35.0	3.35	–1.2	–1.2
182	1133	A	1	H	3	43.0	3.43	–1.1	–1.1
182	1133	A	1	H	3	51.0	3.51	–1.5	–1.5
182	1133	A	1	H	3	59.0	3.59	–1.3	–1.3
182	1133	A	1	H	3	67.0	3.67	–1.0	–1.0
182	1133	A	1	H	3	75.0	3.75	–0.9	–0.9
182	1133	A	1	H	3	83.0	3.83	–0.9	–0.9
182	1133	A	1	H	3	91.0	3.91	–0.9	–0.9
182	1133	A	1	H	3	99.0	3.99	–0.9	–0.9
182	1133	A	1	H	3	107.0	4.07	–1.0	–1.0
182	1133	A	1	H	3	115.0	4.15	–1.4	–1.4
182	1133	A	1	H	3	123.0	4.23	–1.5	–1.5
182	1133	A	1	H	3	131.0	4.31	–1.3	–1.3
182	1133	A	1	H	3	139.0	4.39	–1.0	–1.0
182	1133	A	1	H	3	147.0	4.47	–1.0	–1.0
182	1133	A	1	H	4	3.0	4.53	–1.8	–1.8
182	1133	A	1	H	4	11.0	4.61	–1.9	–1.9
182	1133	A	1	H	4	19.0	4.69	–2.0	–2.0
182	1133	A	1	H	4	27.0	4.77	–2.0	–2.0
182	1133	A	1	H	4	35.0	4.85	–2.0	–2.0
182	1133	A	1	H	4	43.0	4.93	–2.0	–2.0
182	1133	A	1	H	4	51.0	5.01	–2.1	–2.1

Note: Only a portion of this table appears here. The complete table is available in **ASCII format.**

Table T12. Natural gamma-ray measurements from the multisensor track, Site 1133.

Leg	Site	Hole	Core	Type	Section	Interval (cm)	Depth (mbsf)	NGR (cps)
182	1133	A	1	H	1	11.0	0.11	7.73
182	1133	A	1	H	1	27.0	0.27	7.31
182	1133	A	1	H	1	43.0	0.43	6.12
182	1133	A	1	H	1	59.0	0.59	5.65
182	1133	A	1	H	1	75.0	0.75	4.62
182	1133	A	1	H	1	91.0	0.91	5.62
182	1133	A	1	H	1	107.0	1.07	7.08
182	1133	A	1	H	1	123.0	1.23	8.19
182	1133	A	1	H	1	139.0	1.39	8.50
182	1133	A	1	H	2	11.0	1.61	6.39
182	1133	A	1	H	2	27.0	1.77	7.85
182	1133	A	1	H	2	43.0	1.93	9.04
182	1133	A	1	H	2	59.0	2.09	9.08
182	1133	A	1	H	2	75.0	2.25	6.65
182	1133	A	1	H	2	91.0	2.41	9.42
182	1133	A	1	H	2	107.0	2.57	8.92
182	1133	A	1	H	2	123.0	2.73	8.04
182	1133	A	1	H	2	139.0	2.89	8.73
182	1133	A	1	H	3	11.0	3.11	9.15
182	1133	A	1	H	3	27.0	3.27	7.46
182	1133	A	1	H	3	43.0	3.43	7.23
182	1133	A	1	H	3	59.0	3.59	7.35
182	1133	A	1	H	3	75.0	3.75	7.39
182	1133	A	1	H	3	91.0	3.91	11.58
182	1133	A	1	H	3	107.0	4.07	10.27
182	1133	A	1	H	3	123.0	4.23	10.27
182	1133	A	1	H	3	139.0	4.39	7.89
182	1133	A	1	H	4	11.0	4.61	8.27
182	1133	A	1	H	4	27.0	4.77	8.65
182	1133	A	1	H	4	43.0	4.93	10.23
182	1133	A	1	H	4	59.0	5.09	8.58
182	1133	A	1	H	4	75.0	5.25	6.00
182	1133	A	1	H	4	91.0	5.41	8.46
182	1133	A	1	H	4	107.0	5.57	8.89
182	1133	A	1	H	4	123.0	5.73	9.00
182	1133	A	1	H	4	139.0	5.89	7.65
182	1133	A	1	H	5	11.0	6.11	10.58
182	1133	A	1	H	5	27.0	6.27	9.54
182	1133	A	1	H	5	43.0	6.43	10.54
182	1133	A	1	H	5	59.0	6.59	12.15
182	1133	A	1	H	5	75.0	6.75	10.58
182	1133	A	1	H	5	91.0	6.91	10.31
182	1133	A	1	H	5	107.0	7.07	10.04
182	1133	A	1	H	5	123.0	7.23	9.92
182	1133	A	1	H	5	139.0	7.39	12.54
182	1133	A	1	H	6	11.0	7.61	9.50
182	1133	A	1	H	6	27.0	7.77	10.35
182	1133	A	1	H	6	43.0	7.93	10.92
182	1133	A	1	H	6	59.0	8.09	8.54
182	1133	A	1	H	6	75.0	8.25	10.89
182	1133	A	1	H	6	91.0	8.41	10.15
182	1133	A	1	H	6	107.0	8.57	12.73
182	1133	A	1	H	6	123.0	8.73	11.23
182	1133	A	1	H	6	139.0	8.89	12.89
182	1133	A	1	H	7	11.0	9.11	8.89
182	1133	A	1	H	7	27.0	9.27	11.85
182	1133	A	1	H	7	43.0	9.43	11.35
182	1133	B	1	H	1	11.0	0.11	7.12
182	1133	B	1	H	1	27.0	0.27	6.00
182	1133	B	1	H	1	43.0	0.43	8.65
182	1133	B	1	H	1	59.0	0.59	5.12
182	1133	B	1	H	1	75.0	0.75	5.04
182	1133	B	1	H	1	91.0	0.91	5.85
182	1133	B	1	H	1	107.0	1.07	5.81

Notes: NGR = natural gamma ray. Only a portion of this table appears here. The complete table is available in **ASCII format.**

Table T13. Discrete *P*-wave velocity from measurements using PWS1, PWS2, and PWS3, Site 1133.

Leg	Site	Hole	Core	Type	Section	Interval (cm)	Depth (mbsf)	PWS 1, 2, or 3	V_p (km/s)
182	1133	A	1	H	1	12.4	0.12	2	1.5788
182	1133	A	1	H	1	45.6	0.46	1	1.5598
182	1133	A	1	H	1	79.5	0.80	2	1.5897
182	1133	A	1	H	1	80.2	0.80	2	1.5897
182	1133	A	1	H	1	109.5	1.10	1	1.6271
182	1133	A	1	H	2	19.5	1.70	1	1.5808
182	1133	A	1	H	2	57.7	2.08	1	1.5693
182	1133	A	1	H	2	99.0	2.49	1	1.5663
182	1133	A	1	H	2	99.0	2.49	1	1.5693
182	1133	A	1	H	2	140.8	2.91	1	1.5705
182	1133	A	1	H	3	13.5	3.14	1	1.5765
182	1133	A	1	H	3	59.2	3.59	1	1.5912
182	1133	A	1	H	3	94.2	3.94	1	1.5863
182	1133	A	1	H	3	132.1	4.32	1	1.5741
182	1133	A	1	H	4	15.6	4.66	2	1.5015
182	1133	A	1	H	4	59.6	5.10	2	1.5608
182	1133	A	1	H	4	92.3	5.42	2	1.5666
182	1133	A	1	H	4	140.2	5.90	2	1.5690
182	1133	A	1	H	5	15.6	6.16	2	1.5872
182	1133	A	1	H	5	43.8	6.44	1	1.5952
182	1133	A	1	H	5	79.1	6.79	2	1.5678
182	1133	A	1	H	5	110.0	7.10	1	1.5841
182	1133	A	1	H	5	133.6	7.34	2	1.5946
182	1133	A	1	H	6	17.5	7.68	1	1.5977
182	1133	A	1	H	6	51.2	8.01	2	1.6102
182	1133	A	1	H	6	83.7	8.34	1	1.6506
182	1133	A	1	H	6	111.6	8.62	2	1.6477
182	1133	A	1	H	6	142.2	8.92	1	1.5881
182	1133	A	1	H	7	9.6	9.10	2	1.6385
182	1133	A	1	H	7	40.8	9.41	2	1.5685
182	1133	B	1	H	1	48.9	0.49	2	1.5484
182	1133	B	1	H	1	90.7	0.91	2	1.4698
182	1133	B	1	H	1	138.6	1.39	2	1.5965
182	1133	B	1	H	2	16.5	1.67	2	1.5611
182	1133	B	1	H	2	61.1	2.11	2	1.5637
182	1133	B	2	H	1	18.9	2.59	2	1.5681
182	1133	B	2	H	1	51.8	2.92	2	1.5738
182	1133	B	2	H	1	99.0	3.39	2	1.5788
182	1133	B	2	H	1	144.5	3.85	2	1.5655
182	1133	B	2	H	2	17.3	4.07	1	1.5841
182	1133	B	2	H	2	42.5	4.33	2	1.5836
182	1133	B	2	H	2	101.8	4.92	2	1.5715
182	1133	B	2	H	2	137.3	5.27	2	1.5555
182	1133	B	2	H	3	16.8	5.57	1	1.5857
182	1133	B	2	H	3	42.0	5.82	2	1.5566
182	1133	B	2	H	3	74.7	6.15	1	1.5592
182	1133	B	2	H	3	99.9	6.40	2	1.5661
182	1133	B	2	H	3	133.3	6.73	2	1.5479
182	1133	B	2	H	4	7.8	6.98	2	1.5569
182	1133	B	2	H	4	41.4	7.31	2	1.5583
182	1133	B	2	H	4	93.6	7.84	2	1.5679
182	1133	B	2	H	4	134.9	8.25	2	1.5455
182	1133	B	2	H	5	17.8	8.58	2	1.5639
182	1133	B	2	H	5	54.3	8.94	2	1.5611
182	1133	B	2	H	5	91.0	9.31	2	1.5597
182	1133	B	2	H	5	138.6	9.79	2	1.5597
182	1133	B	2	H	6	8.4	9.98	2	1.5148
182	1133	B	2	H	6	52.5	10.43	2	1.5910
182	1133	B	2	H	6	89.1	10.79	2	1.6671
182	1133	B	2	H	7	18.2	11.08	2	1.6217
182	1133	B	2	H	7	52.8	11.43	2	1.5977
182	1133	B	3	H	1	87.6	12.78	2	1.5953
182	1133	B	3	H	1	132.6	13.23	2	1.5855
182	1133	B	3	H	2	15.0	13.55	2	1.6154

Note: Only a portion of this table appears here. The complete table is available in **ASCII format.**

Table T14. Index properties measurements, Site 1133.

Leg	Site	Hole	Core	Type	Section	Top (cm)	Bottom (cm)	Depth (mbsf)	Bulk water content (%)	Dry water content (%)	Bulk density (g/cm^3)	Dry density (g/cm^3)	Grain density (g/cm^3)	Porosity (%)	Void ratio
182	1133	A	1	H	1	71.0	73.0	0.71	35.5	55.1	1.70	1.10	2.67	59.0	1.44
182	1133	A	1	H	2	71.0	73.0	2.21	37.8	60.7	1.66	1.03	2.67	61.3	1.59
182	1133	A	1	H	3	71.0	73.0	3.71	37.3	59.5	1.67	1.05	2.68	60.9	1.56
182	1133	A	1	H	4	70.0	72.0	5.20	38.2	61.9	1.66	1.02	2.69	61.9	1.63
182	1133	A	1	H	5	71.0	73.0	6.71	36.8	58.1	1.69	1.07	2.70	60.5	1.53
182	1133	A	1	H	6	89.0	91.0	8.39	31.5	46.0	1.79	1.22	2.71	55.0	1.22
182	1133	B	1	H	1	79.0	81.0	0.79	32.3	47.8	1.75	1.19	2.66	55.4	1.24
182	1133	B	1	H	2	48.0	50.0	1.98	36.2	56.6	1.70	1.08	2.70	59.9	1.50
182	1133	B	2	H	1	55.0	57.0	2.95	34.8	53.4	1.73	1.13	2.72	58.6	1.42
182	1133	B	2	H	2	55.0	57.0	4.45	38.1	61.5	1.67	1.03	2.72	62.0	1.63
182	1133	B	2	H	3	55.0	57.0	5.95	33.5	50.3	1.74	1.16	2.70	57.0	1.33
182	1133	B	2	H	4	56.0	58.0	7.46	25.5	34.2	1.92	1.43	2.74	47.8	0.91
182	1133	B	2	H	5	57.0	59.0	8.97	32.1	47.4	1.77	1.20	2.70	55.5	1.25
182	1133	B	2	H	6	59.0	61.0	10.49	35.7	55.6	1.70	1.09	2.69	59.4	1.46
182	1133	B	2	H	7	60.0	62.0	11.50	30.0	42.8	1.81	1.27	2.70	53.0	1.13
182	1133	B	3	H	1	117.0	119.0	13.07	30.8	44.5	1.76	1.21	2.57	52.8	1.12
182	1133	B	3	H	2	69.0	71.0	14.09	28.0	39.0	1.82	1.31	2.62	49.9	1.00
182	1133	B	3	H	3	69.0	71.0	15.59	21.8	27.9	1.93	1.51	2.55	41.1	0.70
182	1133	B	3	H	5	67.0	69.0	18.48	29.7	42.3	1.79	1.26	2.62	51.9	1.08
182	1133	B	3	H	6	49.0	51.0	19.80	24.6	32.6	1.93	1.45	2.70	46.2	0.86
182	1133	B	3	H	6	68.0	70.0	19.99	24.7	32.9	1.88	1.42	2.60	45.5	0.84
182	1133	B	4	H	1	69.0	71.0	22.09	29.7	42.2	1.81	1.27	2.68	52.5	1.11
182	1133	B	4	H	2	69.0	71.0	23.59	29.9	42.6	1.81	1.27	2.70	52.9	1.12
182	1133	B	4	H	3	69.0	71.0	25.09	31.7	46.4	1.77	1.21	2.68	54.8	1.21
182	1133	B	4	H	4	69.0	71.0	26.59	32.9	49.1	1.74	1.17	2.66	56.1	1.28
182	1133	B	4	H	5	69.0	71.0	28.09	35.4	54.8	1.71	1.10	2.69	59.0	1.44
182	1133	B	4	H	6	69.0	71.0	29.59	30.5	44.0	1.80	1.25	2.70	53.7	1.16
182	1133	B	4	H	7	69.0	71.0	31.09	28.4	39.6	2.05	1.47	3.41	56.9	1.32
182	1133	B	5	H	1	89.0	91.0	31.79	30.8	44.5	1.79	1.24	2.69	53.9	1.17
182	1133	B	5	H	2	59.0	61.0	32.99	32.7	48.7	1.75	1.18	2.67	55.9	1.27
182	1133	B	5	H	5	89.0	91.0	37.04	32.6	48.3	1.76	1.18	2.68	55.9	1.27
182	1133	B	5	H	6	68.0	70.0	38.33	25.6	34.4	1.90	1.42	2.70	47.5	0.91
182	1133	B	8	X	1	103.0	105.0	51.93	33.6	50.6	1.72	1.14	2.62	56.4	1.29
182	1133	B	8	X	2	82.0	84.0	53.22	34.1	51.8	1.71	1.13	2.61	56.9	1.32
182	1133	B	8	X	3	128.0	130.0	55.18	36.7	58.1	1.66	1.05	2.58	59.4	1.46
182	1133	B	13	X	1	70.0	72.0	85.60	35.1	54.0	1.71	1.11	2.68	58.6	1.41

Note: This table is also available in **ASCII format.**

Table T15. Undrained shear strength measurements, Site 1133.

Leg	Site	Hole	Core	Type	Section	Interval (cm)	Depth (mbsf)	Maximum shear strength (kPa)	Peak (kPa)
182	1133	A	1	H	2	128.6	2.79	4.77	5.82
182	1133	A	1	H	3	122.7	4.23	4.50	5.49
182	1133	A	1	H	4	131.3	5.81	5.85	7.14
182	1133	A	1	H	5	124.5	7.24	7.11	8.67
182	1133	A	1	H	6	126.5	8.77	6.12	7.46
182	1133	A	1	H	7	19.8	9.20	11.79	14.38
182	1133	B	1	H	2	32.9	1.83	4.23	5.16
182	1133	B	2	H	1	130.9	3.71	11.70	14.27
182	1133	B	2	H	2	126.5	5.16	7.65	9.33
182	1133	B	2	H	3	125.7	6.66	9.09	11.09
182	1133	B	2	H	3	125.7	6.66	9.09	11.09
182	1133	B	2	H	4	112.6	8.03	7.47	9.11
182	1133	B	2	H	5	130.4	9.70	6.12	7.46
182	1133	B	2	H	6	72.6	10.63	3.60	4.39
182	1133	B	2	H	7	62.6	11.53	5.67	6.92
182	1133	B	3	H	1	110.6	13.01	8.10	9.88
182	1133	B	3	H	2	120.4	14.60	9.09	11.09
182	1133	B	3	H	3	101.4	15.91	11.61	14.16
182	1133	B	3	H	5	130.0	19.11	18.27	22.28
182	1133	B	3	H	6	111.1	20.42	13.86	16.90
182	1133	B	3	H	7	18.9	21.00	13.77	16.79
182	1133	B	4	H	1	108.3	22.48	6.39	7.79
182	1133	B	4	H	3	93.1	25.33	17.73	21.62
182	1133	B	4	H	4	131.8	27.22	49.68	60.59
182	1133	B	4	H	5	98.6	28.39	38.16	46.54
182	1133	B	4	H	6	140.3	30.30	7.20	8.78
182	1133	B	5	H	1	137.6	32.28	14.13	17.23
182	1133	B	5	H	5	114.2	37.29	4.95	6.04
182	1133	C	1	H	2	132.5	2.83	4.95	6.04
182	1133	C	1	H	3	127.8	4.28	6.93	8.45
182	1133	C	2	H	1	133.9	7.14	6.66	8.12
182	1133	C	2	H	2	99.5	8.30	13.50	16.47
182	1133	C	2	H	3	98.4	9.78	18.00	21.95
182	1133	C	2	H	4	125.8	11.56	10.44	12.73
182	1133	C	2	H	5	118.7	12.99	15.03	18.33
182	1133	C	2	H	6	92.8	14.23	13.23	16.14
182	1133	C	3	H	1	138.0	16.68	8.82	10.76
182	1133	C	3	H	2	104.7	17.85	24.03	29.31
182	1133	C	3	H	3	124.2	19.54	6.84	8.34
182	1133	C	3	H	4	117.6	20.98	10.89	13.28
182	1133	C	3	H	5	119.6	22.50	20.34	24.81
182	1133	C	4	H	1	113.0	25.93	18.45	22.50
182	1133	C	4	H	1	113.0	25.93	18.45	22.50
182	1133	C	4	H	2	113.8	27.44	11.88	14.49
182	1133	C	4	H	3	116.7	28.97	1.89	2.31
182	1133	C	4	H	4	110.4	30.40	2.52	3.07
182	1133	C	4	H	5	113.5	31.93	3.69	4.50
182	1133	C	4	H	5	113.5	31.93	3.69	4.50
182	1133	C	4	H	6	115.6	33.46	4.86	5.93
182	1133	C	6	H	1	130.0	45.10	7.11	8.67
182	1133	C	6	H	2	120.7	46.51	23.58	28.76

Note: This table is also available in **ASCII format.**

Table T16. Thermal conductivity measurements, Site 1133.

Leg	Site	Hole	Core	Type	Section	Interval (cm)	Depth (mbsf)	Thermal conductivity (W/[m·K])
182	1133	A	1	H	3	75.0	3.75	0.986
182	1133	B	2	H	3	75.0	6.15	1.108
182	1133	B	3	H	3	75.0	15.65	1.213
182	1133	B	3	H	6	75.0	20.06	1.165
182	1133	B	4	H	1	71.0	22.11	1.143
182	1133	B	4	H	3	71.0	25.11	1.212
182	1133	B	5	H	3	44.0	33.59	1.186
182	1133	B	8	X	3	76.0	54.66	1.015
182	1133	B	13	X	1	76.0	85.66	1.011

Note: This table is also available in **ASCII format.**